

NPS ARCHIVE
1997.12
ALBA, A.

NAVAL POSTGRADUATE SCHOOL MONTEREY, CALIFORNIA



THESIS

THE USE OF RIGID POLYURETHANE FOAM AS A LANDMINE BREACHING TECHNIQUE

by

Albert L. Alba

December 1997

Thesis Advisor:

X. K. Maruyama

Thesis
A33456

Approved for public release; distribution is unlimited.

DUDLEY KNOX LIBRARY
NAVAL POSTGRADUATE SCHOOL
MONTEREY CA 93943-5101

REPORT DOCUMENTATION PAGE

Form Approved OMB No. 0704-0188

Public reporting burden for this collection of information is estimated to average 1 hour per response, including the time for reviewing instruction, searching existing data sources, gathering and maintaining the data needed, and completing and reviewing the collection of information. Send comments regarding this burden estimate or any other aspect of this collection of information, including suggestions for reducing this burden, to Washington Headquarters Services, Directorate for Information Operations and Reports, 1215 Jefferson Davis Highway, Suite 1204, Arlington, VA 22202-4302, and to the Office of Management and Budget, Paperwork Reduction Project (0704-0188) Washington DC 20503.

| | | | | | |
|--|--|---|----------------------------------|---|--|
| 1. AGENCY USE ONLY (Leave blank) | | 2. REPORT DATE December 1997 | | 3. REPORT TYPE AND DATES COVERED Master's Thesis | |
| 4. TITLE AND SUBTITLE TITLE OF THESIS. THE USE OF RIGID POLYURETHANE FOAM AS A LANDMINE BREACHING TECHNIQUE | | | | 5. FUNDING NUMBERS | |
| 6. AUTHOR(S) Alba, Albert L. | | | | | |
| 7. PERFORMING ORGANIZATION NAME(S) AND ADDRESS(ES) Naval Postgraduate School Monterey CA 93943-5000 | | | | 8. PERFORMING ORGANIZATION REPORT NUMBER | |
| 9. SPONSORING/MONITORING AGENCY NAME(S) AND ADDRESS(ES) NSAP, Office of Naval Research; Office of Munitions, OUSD | | | | 10. SPONSORING/MONITORING AGENCY REPORT NUMBER | |
| 11. SUPPLEMENTARY NOTES The views expressed in this thesis are those of the author and do not reflect the official policy or position of the Department of Defense or the U.S. Government. | | | | | |
| 12a. DISTRIBUTION/AVAILABILITY STATEMENT Approved for public release; distribution is unlimited. | | | | 12b. DISTRIBUTION CODE | |
| 13. ABSTRACT (maximum 200 words) The results of a feasibility test using Rigid Polyurethane Foam (RPF) as an operational anti-personnel mine counter-mine technique are presented. RPF, at a given density and thickness, can withstand the explosive effects of anti-personnel blast mines and mitigate or neutralize the effects of surface laid anti-vehicular mines. A 12-inch thick, 4 pound per cubic foot foam block completely contained a 10 gram explosive charge of PETN while a 30-inch foam block with the same density contained a 30 gram charge. A 24-inch thick pad supported 50 passes of an M88A2 Recovery Vehicle, crushing the foam no more than 2-3 inches throughout the length of a 56 foot foam roadway. Underneath this roadway, simulated land mines set at 14 psi were not detonated by the passage of an M88A2 and a HMMWV. Our experiments indicate that RPF can provide additional traction in muddy conditions and set-off explosives connected to trip wires. The pressure and trafficability experiments were conducted at the Waterways Experiment Station, Vicksburg, MS in July-August 1997, and the explosive experiments were conducted at the Energetic Materials Research and Testing Center (EMRTC) of the New Mexico Institute of Mining and Technology, Socorro, NM in August and October 1997. | | | | | |
| 14. SUBJECT TERMS Explosives, Landmine, Rigid Polyurethane Foam, Countermine | | | | 15. NUMBER OF PAGES 77 | |
| | | | | 16. PRICE CODE | |
| 17. SECURITY CLASSIFICATION OF REPORT Unclassified | 18. SECURITY CLASSIFICATION OF THIS PAGE Unclassified | 19. SECURITY CLASSIFICATION OF ABSTRACT Unclassified | 20. LIMITATION OF ABSTRACT UL | | |

NSN 7540-01-280-5500

Standard Form 298 (Rev. 2-89)
Prescribed by ANSI Std. Z39-18 298-102

Approved for public release; distribution is unlimited.

**THE USE OF RIGID POLYURETHANE FOAM AS A LANDMINE
BREACHING TECHNIQUE**

Albert L. Alba
Captain, United States Army
B.S., United States Military Academy, 1989

Submitted in partial fulfillment
of the requirements for the degree of

MASTER OF SCIENCE IN APPLIED PHYSICS

from the

**NAVAL POSTGRADUATE SCHOOL
December 1997**

NPS ARCHIVE

1997.12

ALBA, A.

Thes/c
A3343
C.2

ABSTRACT

The results of a feasibility test using Rigid Polyurethane Foam (RPF) as an operational anti-personnel mine counter-mine technique are presented. RPF, at a given density and thickness, can withstand the explosive effects of anti-personnel blast mines and mitigate or neutralize the effects of surface laid anti-vehicular mines. A 12-inch thick, 4 pound per cubic foot foam block completely contained a 10-gram explosive charge of PETN while a 30-inch foam block with the same density contained a 30-gram charge. A 24-inch thick pad supported 50 passes of an M88A2 Recovery Vehicle, crushing the foam no more than 2-3 inches throughout the length of a 56 foot foam roadway. Underneath this roadway, simulated land mines set at 14 psi were not triggered by the passage of an M88A2 and a HMMWV. Our experiments indicate that RPF can provide additional traction in muddy conditions and set-off explosives connected to trip wires. The pressure and trafficability experiments were conducted at the Waterways Experiment Station, Vicksburg, MS in July-August 1997, and the explosive experiments were conducted at the Energetic Materials Research and Testing Center (EMRTC) of the New Mexico Institute of Mining and Technology, Socorro, NM in August and October 1997.

TABLE OF CONTENTS

| | |
|--|----|
| I. INTRODUCTION..... | 1 |
| II. BACKGROUND..... | 3 |
| A. RIGID POLYURETHANE FOAM..... | 3 |
| B. PREVIOUS WORK DONE BY SANDIA NATIONAL LABORATORIES... | 4 |
| III. EXPERIMENT..... | 9 |
| A. GENERAL..... | 9 |
| B. TRAFFICABILITY AND PRESSURE EXPERIMENTS..... | 9 |
| C. EXPLOSIVE EXPERIMENTS..... | 22 |
| IV. ANALYSES..... | 37 |
| A. WATERWAYS EXPERIMENTS..... | 37 |
| B. EXPLOSIVE EXPERIMENTS..... | 44 |
| V. CONCLUSIONS AND RECOMMENDATIONS..... | 51 |
| A. CONCLUSIONS..... | 51 |
| B. RECOMMENDATIONS..... | 52 |
| VI. OTHER CONSIDERATIONS AND APPLICATIONS..... | 53 |
| A. UNDERWATER EXPLOSIVE CAVITY FORMATIONS..... | 53 |
| B. ENERGY ABSORPTION PROPERTIES OF RPF..... | 53 |
| C. LOGISTICAL CONSIDERATIONS..... | 54 |
| LIST OF REFERENCES..... | 55 |
| BIBLIOGRAPHY..... | 57 |
| INITIAL DISTRIBUTION LIST..... | 59 |

LIST OF FIGURES

| | |
|---|----|
| 1. Basic formation of polyurethanes, polyol + diisocyanate from Ref. [10]..... | 3 |
| 2. Blast cavity diameters from surface and embedded shots from Ref. [11] | 7 |
| 3. Set-up for Trafficability Tests..... | 11 |
| 4. Mine and Pressure Cell Layout..... | 12 |
| 5. Set-up for Roadway Experiments..... | 13 |
| 6. Foam wear from M88A2 and HMMWV..... | 15 |
| 7. Results of Roadway Experiments..... | 15 |
| 8. Set-up for M88A2 drawbar-pull experiments..... | 17 |
| 9. Dispensing foam into Water logged M88A2 ruts to investigate traction effects..... | 18 |
| 10. Foam-filled ruts for M88A2 traction test..... | 19 |
| 11. HMMWV drawbar pull experiments. This HMMWV is pulling a water truck located 20 meters to its rear..... | 19 |
| 12. M88A2 conducting traction tests..... | 20 |
| 13. Foam damage during traction tests..... | 21 |
| 14. Schematic for Land Experiments | 23 |
| 15. Ground set-up for experiments..... | 23 |
| 16. PETN explosives used in experiments..... | 24 |
| 17. Frame used to mold foam blocks..... | 25 |
| 18. Decker Foam Machine..... | 26 |
| 19. PETN set-up for explosive cavity experiments..... | 28 |
| 20. Set-up of Experiment L1..... | 28 |
| 21. Sketch of the explosive effects on an RPF block..... | 31 |
| 22. Entry cavity for Experiment L1..... | 31 |
| 23. Exit cavity for Experiment L1..... | 32 |
| 24. Ground crater from Experiment L1..... | 32 |
| 25. Entry Cavity for Experiment L9..... | 33 |
| 26. Exit Cavity for Experiment L9 (No perforation)..... | 33 |

| | |
|--|----|
| 27. Ground Crater from Experiment L9..... | 34 |
| 28. Dispensing Foam into damaged section..... | 35 |
| 29. Top Surface of a Repaired block of foam..... | 36 |
| 30. Cross section of repaired block of foam..... | 36 |
| 31. Dry Surface drawbar-pull test on M88A2..... | 38 |
| 32. Wet surface drawbar-pull test on M88A2..... | 39 |
| 33. Foam surface drawbar-pull test on M88A2..... | 39 |
| 34. Dry Surface drawbar-pull test on HMMWV..... | 40 |
| 35. Wet Surface drawbar-pull test on HMMWV..... | 40 |
| 36. Foam Surface drawbar-pull test on HMMWV..... | 41 |
| 37. Change in maximum pressure versus pass number..... | 44 |
| 38. Cavity Prediction for 4 lb/ft ³ based on Surface and Embedded Data (C-4)..... | 46 |
| 39. Comparison between Ground Shots and Surface and Embedded Shots..... | 46 |
| 40. Charge Mass vs. Blast Cavity Diameter and Depth..... | 49 |
| 41. Sketch of a repaired foam block..... | 50 |
| 42. Set-up for the Underwater Explosive Experiments | 53 |

LIST OF TABLES

| | |
|---|----|
| 1. Matrix for Explosive Cavity Formation Experiments | 27 |
| 2. Results of Explosive Cavity Formation Experiments..... | 30 |
| 3. Summary of anti-tank mines neutralized due to 60 cm application of foam..... | 42 |
| 4. Effects of M88A2 and HMMWV on Anti-personnel (Pressure Fuzed) mines..... | 42 |
| 5. Effects of M88A2 and HMMWV on Anti-personnel (Tripwire Fuzed) mines..... | 43 |
| 6. Predicted and Actual Cavity Results for 4 lb/ft ³ foam..... | 45 |
| 7. Comparison of Cavity Diameters and Possible Edge Effects..... | 48 |
| 8. Predicted values for Cavity Depth and Cavity Diameter for 4 lb/ft ³ foam..... | 48 |

LIST OF ACRONYMS AND ABBREVIATIONS

| | |
|-------|---|
| EMRTC | Energetic Materials and Research Center |
| HMMWV | High Mobility Multi-Purpose Wheeled Vehicle |
| MDI | Diphenylmethane Diisocyanate |
| MSDS | Material Safety Data Sheet |
| NCFI | North Carolina Foam Industry |
| RPF | Rigid Polyurethane Foam |
| SNL | Sandia National Laboratories |
| WES | Waterways Experiment Station |

ACKNOWLEDGEMENT

I would like to acknowledge the financial support of the Navy Science Assistance Program of the Office of Naval Research for providing the expenses for my experience tour at Sandia National Laboratories, Albuquerque, NM.

Special thanks are due to the entire Exploratory Sensors and Fuzing Department for their patience and support during my work at Sandia National Laboratories. The experiments at SNL were conducted under the funding provided jointly by the U.S. Department of Energy (DOE) and the Office of the Undersecretary of Defense, Office of Munitions, (OUSD(OM)).

I also want to thank Prof. Xavier Maruyama and Dr. Ronald Woodfin for their guidance during the work in performing my thesis. I would also like to thank Peter Rand (SNL), Charlie Schmidt (LATA), George Mason (WES), Ken Hall (WES), Brad Hance (SNL), David Faucett (SNL), Bernie Gomez (SNL), Ed Jones (SNL), and Terese Gabocy (EMRTC), without whose help, technical assistance, and advice, this thesis would not be possible.

I. INTRODUCTION

Mines, both anti-tank and anti-personnel, have been combat multipliers in past and present battlefields. When properly employed, mines can drastically reduce a unit's ability to maneuver its forces and synchronize its efforts on the battlefield. Currently, our land forces have breach in-stride techniques and countermine systems that can reduce a 300-meter long obstacle within ten minutes, but these techniques and weapon systems are slowly becoming obsolete against the rapidly evolving mine technology and techniques. Harry Hambric [Ref. 4] contends that the United States has made very little countermine progress since World War II, instead, the focus has been on developing fuzing, lethality, and emplacement technologies. This study presents new results using Rigid Polyurethane Foam (RPF) to improve current breaching techniques. The scope of this study is centered on anti-personnel mines, however this report also includes results of experiments that can be extended to anti-tank mines.

The purpose of this study is to determine if rigid polyurethane foam can be used to either neutralize or efficiently attenuate the explosive effects of surface or subsurface laid anti-personnel mines. It will also determine if the foam is a viable system for operational use on the modern day battlefield. Feasibility experiments in the areas of trafficability, traction effects, trip wire reduction, foam repair, and explosive cavity formations will provide information to determine the foam's applicability in military operations. One possible application is to spray the foam on a minefield and allow a combat unit to continue through the obstacle field with speed and avoid losses to the covering enemy unit. Rigid Polyurethane Foam could also be used as a temporary walkway as part of humanitarian efforts to protect civilian populations from mines left behind after a conflict.

Chapter I will introduce the purpose of this study. Chapter II will discuss the properties of Rigid Polyurethane Foam and discuss previous work that has been done by Sandia National Laboratories. Chapter III will describe the experimental set-up, conduct, and results of the feasibility experiments conducted by Waterways Experiment Station, MS, and Sandia National Laboratories. Chapter IV is dedicated to the analysis of the

results from Chapter III, and Chapter V will discuss the conclusions of this study. Chapter VI will discuss other areas of consideration such as underwater explosive effects on foam, energy absorption properties of the foam, and logistical issues regarding the foam's delivery package and performance in all weather conditions.

II. BACKGROUND

A. RIGID POLYURETHANE FOAM (RPF)

The RPF chosen for these feasibility experiments, NCFI 811-91, is a two-part liquid which can expand up to 60 times its original volume. The amount of expansion will depend on the desired strength of the foam. Because of this considerable volume expansion, this foam can be transported in minimum bulk for possible military applications. The two chemicals are 1,1-Dichloro-1-fluoroethane ($\text{CH}_3\text{CCl}_2\text{F}$ or HCFC-141b) and Polymethylenepolyphenylisocyanate (Polymeric MDI). The first chemical is the Polyol resin and the second chemical is the isocyanate. The mix ratio of the chemicals by volume is one part resin to one part isocyanate. The mix ratio by weight is 100 parts resin to 106 parts isocyanate. It has a cream time of 55-65 seconds and a rise time of 3-4 minutes [Ref. 7, 8].

Polyurethanes are formed from the reaction of a polyol with an isocyanate. The polyol, which means multiple alcohols or multiple OH groups, reacts with isocyanate, which is the N-C-O combination of atoms. When these two monomers combine, a more stable molecular structure results from the molecular rearrangement. Figure 1 shows the basic reaction to form polyurethanes [Ref. 12:p. 232]. R is usually a multifunctional polyether but can also be a small organic group while R' is usually a large aromatic group. Diisocyanate is a type of chemical compound that has two isocyanate groups [Ref. 12:p. 232].

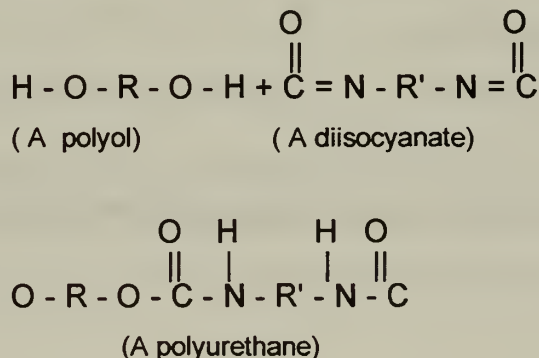


Figure 1. Basic formation of polyurethanes, polyol + diisocyanate from Ref. [12].

Rigid polyurethane foams are produced from the reaction of multifunctional polyols and multifunctional, polymeric isocyanates. RPF is highly crosslinked and has densities ranging from 5 to 15 lb/ft³.

RPF has been used in a variety of applications, such as in the automotive and building industries, but it has been primarily used for thermal insulation, specifically for frozen containers fitted for trains, trucks, aircraft, and ships. In the automotive industry, RPF is used to fill longitudinal runners, motors, and trunk hoods in order to provide additional stiffening. The building industry uses RPF to fill gaps between door casings and walls [Ref. 5:p. 259].

B. PREVIOUS WORK DONE BY SANDIA NATIONAL LABORATORIES

1. General

Dr. Ronald Woodfin of the Exploratory Sensors and Fusing Department of Sandia National Laboratories conducted extensive experiments on RPF from November 1995 through February 1996. His results are contained in SAND96-2841. This Phase I report focuses on the "development of a foam that can neutralize mines and barriers and allow the safe passage of amphibious landing craft and vehicles" [Ref. 13: Abstract]. Phase I concentrated on the following areas:

- Laboratory characterization of foam properties
- Field experiments with prefabricated foam blocks in order to determine its capability to carry military traffic
- Flammability characteristics
- Response to bullet impact
- Toxicity
- Explosive cavity formation from surface and subsurface shots

2. Summary of Results

a. Foam Properties

Peter Rand [Ref. 10], a foam expert from Sandia National Laboratories, conducted the foam property tests and determined that the compressive strength of the foam selected for the Phase I experiments, NCFI 811-91, increases rapidly with increasing density. He also noted that the foam demonstrated lower strength in the perpendicular to rise direction, it would have higher properties in the parallel to rise direction [Ref. 10]. NCFI 811-91 was also selected for the experiments because of the good foam quality that was produced after water immersion. The other foam materials, such as PP 475-20 and Stathane 4802 W, either shrank, had poor quality cell structure, or were brittle [Ref. 9]. Sandia selected a foam that could be used to create a passageway over the obstacles in the shallow surf zone and the beach.

b. Trafficability Experiments on Pre-fabricated Foam Blocks

Trafficability experiments were conducted using 54-inch cube foam blocks with 2, 4, and 6 lb/ft³ densities. An M60 Main Battle Tank, M110 8-inch self propelled Howitzer, 3.5 ton Light truck, and a 6 X 6 cargo truck were used to determine if the foam could adequately carry military traffic. The 2 pcf foam block had a 12-inch rut after 8 to 12 passes by a tracked vehicle while the 4 pcf foam carried 36 to 163 passes of a tracked vehicle before it suffered a 12-inch rut. Sandia concluded that moderate density RPF foams, 2.5 to 3.5 pcf for tracked vehicles, will adequately carry military traffic during the first days of an amphibious assault [Ref. 13:p. xi].

c. Flammability Characteristics

Experiments were conducted using 2 and 4 lb/ft³ foam. In both cases, once the initiating heat was removed, the foam began to self-extinguish. The foam did not develop a flash fire and burned very much like light wood [Ref. 13:p. xi].

d. *Response to Bullet Impact*

Experiments were conducted using rifle caliber small arms on 2 lb/ft³. The bullets slowed down and tumbled in the foam without causing considerable damage. High explosive/point detonating fused projectiles, such as the 30 mm Cannon caliber perforated the 2 lb/ft³ foam, but the projectile did not detonate. The same type of projectile detonated in a 4 lb/ft³ foam and caused moderate damage [Ref. 11:p. xii].

e. *Toxicity*

Melecita Archuleta and William Stocum [Ref. 1] conducted the toxicity evaluation and hazard review for rigid foam and concluded that there is no significant health hazard expected during the normal use or deployment of the foam, but there is a possibility for thermal decomposition at temperatures below ignition, which would result in the generation of toxic isocyanate vapors and other toxic vapors such as Freon-12. These vapors would only be significant to individuals operating near the foam during the foaming process. The deployment of foam in well ventilated areas prevents any asphyxiation hazard due to oxygen depletion.

Archuleta and Stocum also contend that a hazardous situation can occur in the event of a partial deployment of the foam in which only the isocyanate component of RPF is released. This component consists of toxic polymeric isocyanates which can severely irritate the tissues of the mucous membranes and upper respiratory tract. The resin component by itself does not pose a hazardous situation [Ref. 1].

f. *Explosive Cavity Formation from Surface and Subsurface shots*

Explosive experiments were conducted using 10, 100, and 1,000 gram C-4 charges in both 2 and 4 lb/ft³ foam. Charges were either placed on the top surface or interior of the foam blocks. The results of these explosive experiments were accurately predicted by the work of Cooper and Kurowski in 1975.

Figure 2 , [Ref. 13:p. 43], shows the data of Cooper and Kurowski as well as the new data points from the Sandia experiments conducted in 1995. The original work by Cooper and Kurowski is denoted by the X for the 2 lb/ft³ foam and the Δ for the 14 lb/ft³ foam.

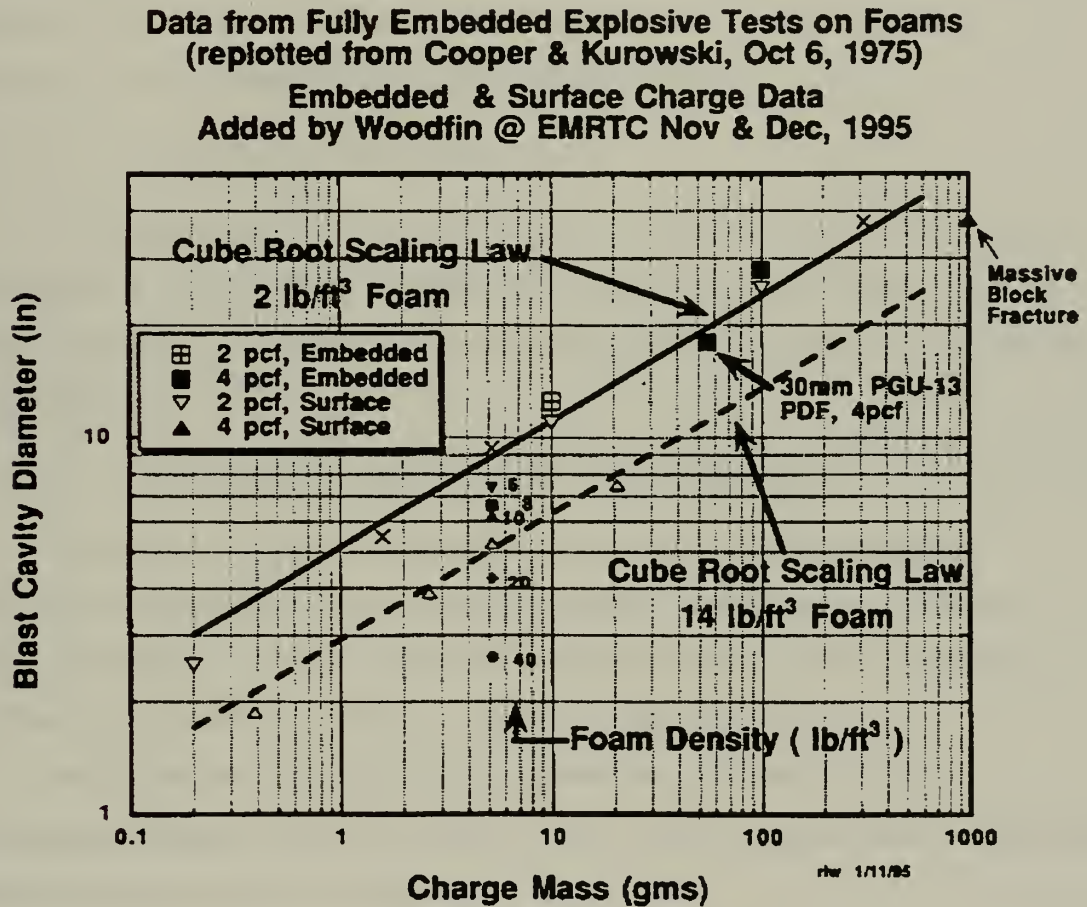


Figure 2. Blast cavity diameters from surface and embedded shots from Ref. [11] conducted by Cooper, Kurowski, and Woodfin. The solid line depicts the 2 lb/ft³ foam while the dashed line depicts the 14 lb/ft³. The prediction of the foam densities (6, 8, 10, 20, and 40 lb/ft³) were predicted by Cooper and Kurowski in 1976.

III. EXPERIMENTS

A. GENERAL

The feasibility experiments were conducted at two locations. The initial experiments were conducted with the Waterways Experiment Station, Vicksburg, MS at Duckport, LA while the explosive tests were conducted with Sandia National Laboratories, Albuquerque, NM, at EMRTC, Socorro, NM.

1. Waterways Experiment Station

Waterways conducted a Concept Evaluation Program in order to determine the trafficability of a foam roadway, the ability of the foam to distribute the load of a static and moving vehicle, the effects of laying foam on trip wires, and finally the effects on sub-surface laid mines.

2. Energetic Materials Research and Training Center

The Sandia experiments concentrated on the explosive effects on Rigid Polyurethane Foam blocks. Failure criteria of the foam based on density, explosive charge, and foam thickness were explored. The final experiments were conducted to determine the possibility and efficiency of repairing damaged blocks.

Both experiments were part of an integrated plan with Sandia National Laboratories playing the lead role. Because these were operational feasibility tests, mixed English and metric units are reported.

B. TRAFFICABILITY AND PRESSURE EXPERIMENTS

All trafficability and pressure experiments were conducted at Duckport, LA. These experiments took place between 25 July - 07 August 1997.

1. Trafficability Tests

These experiments were conducted in order to investigate the foam's ability to carry military traffic. A tracked vehicle, M88A2 Hercules Tank Retriever, and a wheeled

vehicle, M998 High Mobility Multi-purpose Wheeled Vehicle (HMMWV), were used for these tests. The M88A2 weighed 138,000 lb and was fitted with an M60 track which produced a contact pressure against the road bed of 17.4 psi. The HMMWV weighed 9,490 lb with a front tire pressure of 25 psi and a rear tire pressure of 35 psi. The contact pressures on the ground were 20 psi and 26 psi respectively.

a. Set-up

An RPF roadway with dimensions, 51' X 26' X 2' was constructed on a flat plastic clay soil surface. Figure 3 is a picture of the final configuration of the foam roadway. The top surface does not have a flat surface because of operational limitations of the foam dispensing machine. The foam dispensing machine was a Decker Industries commercial model applicable to the building industry. The machine can only dispense foam at a maximum rate of 90 lb/min, which is not quick enough to dispense large quantities of foam in the required time for an in-stride breach. In order to construct the 24-inch thick roadway, the foam had to be dispensed in approximately four layers with each layer no more than 6 inches thick. When the layers were poured larger than six inches thick, the internal temperature in the foam increased. This heat buildup caused the foam to split.

Figure 4 shows a schematic of the instrumentation layout and respective paths of the M88A2 and HMMWV. In order to use the roadway for both vehicles, the M88A2's right track traversed over the HMMWV's right wheel path. This method left two clear lanes for the vehicles.



Figure 3. Set-up for Trafficability Tests. Note that the roadway does not have a flat upper surface. The undulations were caused by the uneven rising of the foam. This 24" thick roadway was poured in four separate layers. Each layer was between 5-7 inches thick.

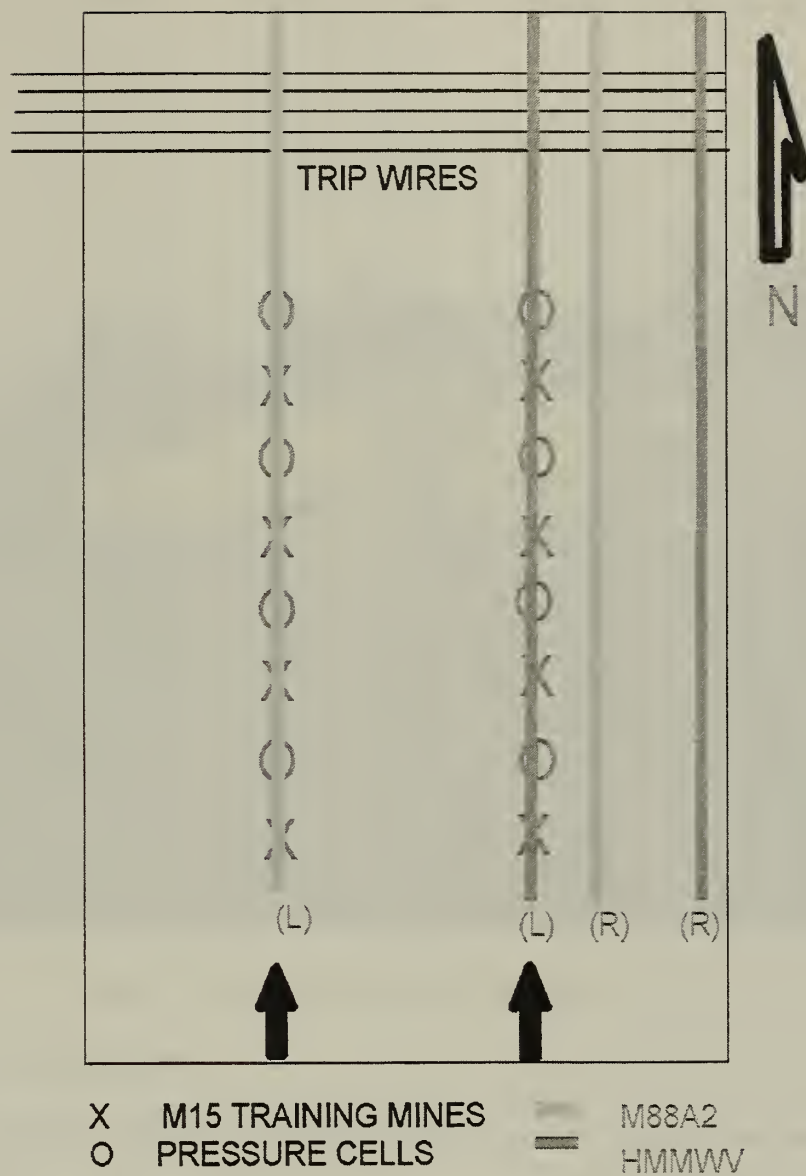


Figure 4. Mine and Pressure Cell Layout. The M15 training mines were employed to simulate anti-tank mines. The pressure cells were located close enough to the mines in order to provide pressure readings after each vehicular pass.

Figure 5 shows the paths taken by the two vehicles. The large ruts were made by the M88A2 while the HMMWV's left wheels crossed over the foam in between the M88A2's path.

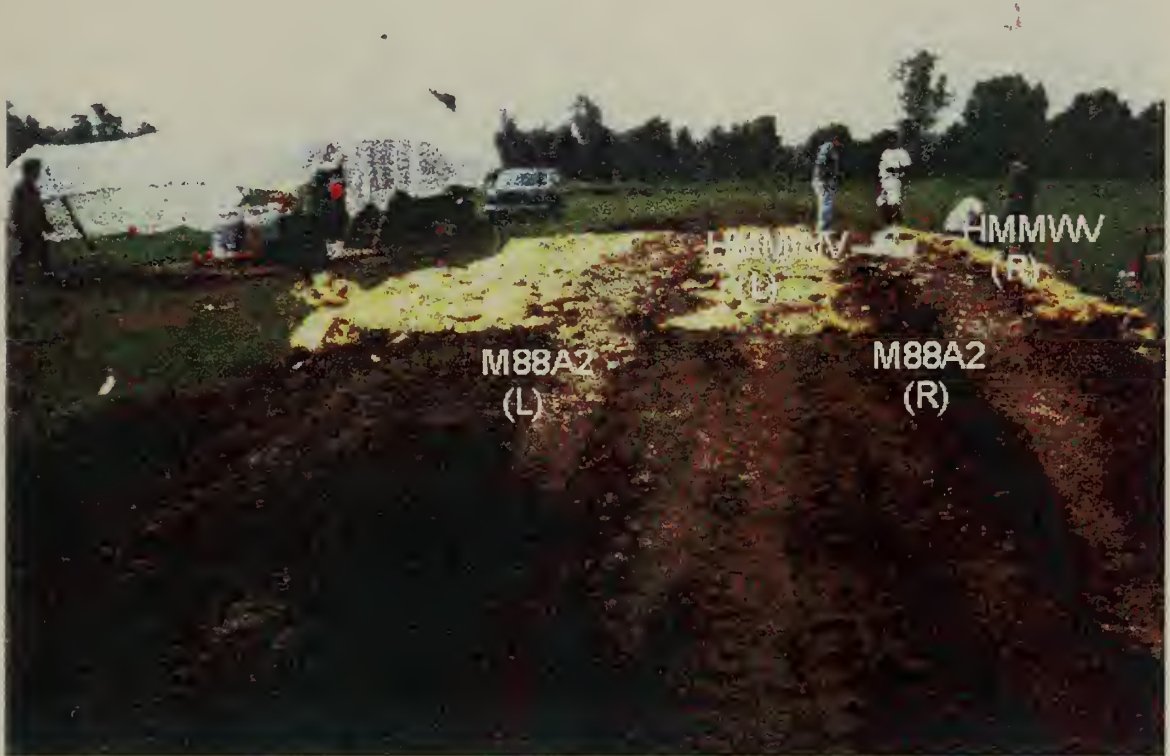


Figure 5. Set-up for Roadway Experiments.

b. Experiment

The M998 HMMWV and M88A2 Tank Retriever were driven over the 24-inch deep, 4 lb/ft³ foam roadway for a total of 50 passes each. The HMMWV initially made 5 passes over its predetermined path. Indentation measurements of the foam were taken after each pass, which was one length of the roadway in the forward direction. The M88A2 then made its first 10 passes, which consisted of 5 forward and 5 reverse passes over the roadway. Indentation measurements were taken after the first five passes followed by measurements after every fifth pass. The HMMWV completed its remaining 45 passes followed by 40 more passes of the M88A2 .

c. Results

After the first five passes, the HMMWV vehicle barely indented the foam. In some areas where the foam was slightly higher, small cracks developed. After 50 passes, the foam was indented no more than 1 inch. These indentations were measured on the left track which was not affected by the M88A2. Figure 6 shows the indentation marks of the HMMWV on the upper right foam path.

The M88A2's first pass created an indentation up to an inch in depth in some portions of foam. After the second pass, the M88A2 began to pack the foam underneath the tracks and the debris began to settle on top of the worn surface. After 50 passes, the M88A2 crushed the foam between 2-3 inches throughout the length of the roadway. Figure 6 shows the rut created by the M88A2 and the slight indentation created by the HMMWV. Figure 7 shows another view of the damaged roadway as well as the chunks of debris that are compacted in the path.

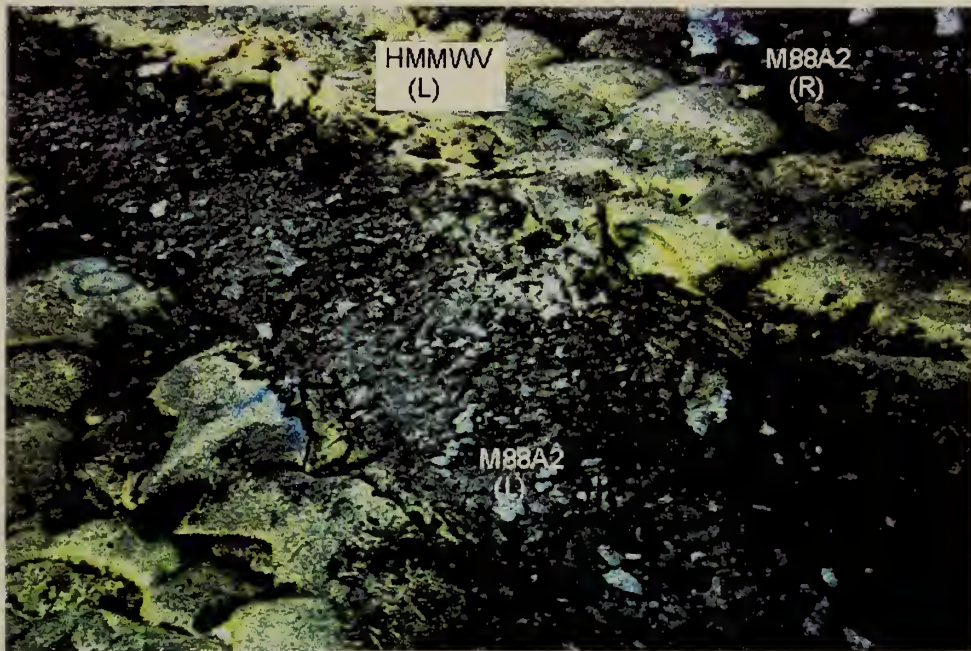


Figure 6. Foam wear from the M88A2 and HMMWV. Note that the HMMWV barely indented the foam while the M88A2 created two large ruts.



Figure 7. Results of Roadway Experiments. The deep ruts were created by the left and right tracks of the M88A2. The HMMWV left the discoloration in the center of the roadway.

2. Trip Wire Experiments

a. Set-up

Figure 3 shows the set-up of the trip wires on the northern end of the roadway. Three of the trip-wires were M-1, 7 lb pull devices while the remaining two were string tension potentiometers. Each wire was anchored on one end to a wooden stake while the other end was attached to a tripping mechanism set at 7 lb. The wires were approximately two inches above the ground.

b. Experiments

The foam was poured into the trip wire area with a west to east fill pattern. The goal was to achieve a total foam depth of 24 inches. Due to limitations of the foam machine, this depth had to be achieved in multiple layers. An initial layer of 6 inches was followed by three more 6-inch layers. Additional layers were applied only after the bottom layer became tack-free. Dirt berms about 18 inches in height were constructed along the edges of the minefield in order to help confine the flow of the foam.

c. Results

At the front end, the wire remained embedded in the foam. The expansion of the foam caused the wires to rise. The expansion continued to the very end of the pour. Initial results indicated that the foam stretched the wire 8-10 inches.

These results were not very conclusive because of the manner at which the foam was applied. The foam started to expand from the western edge, but the flow of the rising foam was towards the eastern edge. This created a gradual slope wherein the eastern edge was approximately 6 inches thicker than the western edge.

3. Traction Experiments

a. Set-up

An M88A2 is configured to pull another M88A2 located 20 meters to its rear. A bulldozer was used as the brake vehicle.

b. Experiments

Initial traction tests (drawbar pull experiments) for the M88A2 and HMMWV were conducted on dry surface. These experiments were then repeated on a watered down surface which simulated 2 inches of rain. The final traction tests involved spraying 5 - 8 inches of foam in the watered down ruts. After allowing the foam to cure for one hour, the lead M88A2 ran over the foam with the other M88A2 in tow. Figures 8, 9, and 10 show the set-up for the traction tests. Measurements were taken to determine if the foam provided any additional traction for the pulling vehicle.

Similar traction experiments were conducted with the HMMWV. The HMMWV pulled a water truck with a 5-ton truck as a break vehicle. Instead of just filling in the rut created by the repeated passes of the HMMWV, 3-5 inches of foam was sprayed over the entire roadway. This procedure was modified for the HMMWV in order to ensure that the wheels would maintain contact with the foam throughout the entire length of the road. Figure 11 shows the HMMWV pulling the water truck while driving on the foamed roadway.



Figure 8. Set-up for M88A2 drawbar-pull experiments.



Figure 9. Dispensing foam into water logged M88A2 ruts to investigate traction effects.



Figure 10. Foam-filled ruts for M88A2 traction test. The foam was allowed to cure for one hour before the experiments were conducted.



Figure 11. HMMWV drawbar pull experiments. This HMMWV is pulling a water truck located 20 meters to its rear.

c. Results

The M88A2 initially crushed the foam before it completely churned up the entire foam in the ruts, Figure 11 and 12. The foam was not as hard as the foam placed on dry land. It was easier to compress because of its lower density. The foam also had a much lower measured internal temperature, 174 ° F, because of the presence of water in the rut. Without water, the measured internal temperature in the foam is greater than 400° F. The drawbar pull experiments determined that the foam did not provide any additional traction for the pulling vehicle.

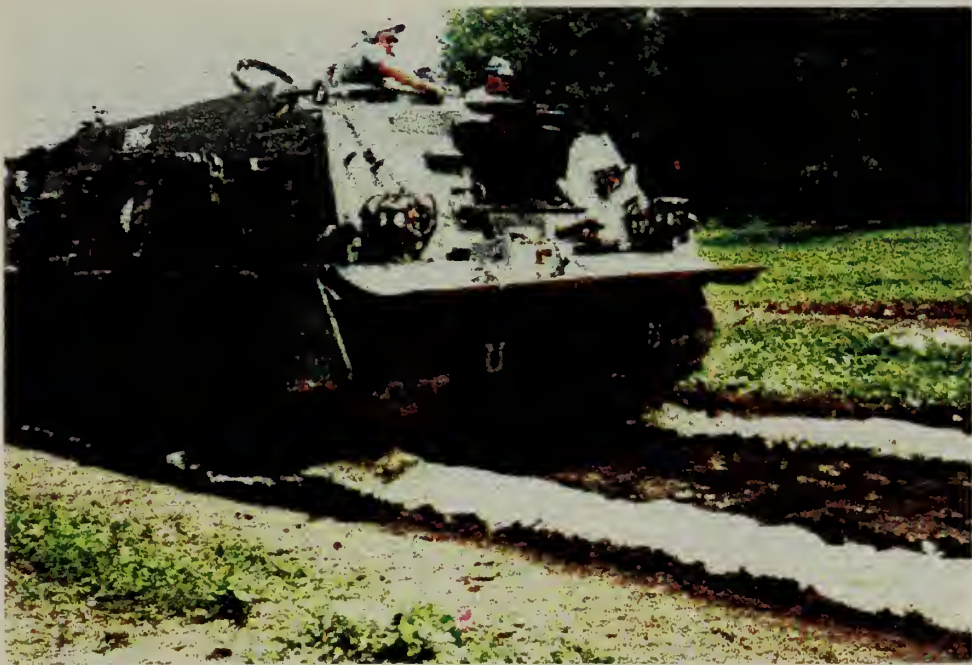


Figure 12. M88A2 conducting traction tests. The foam immediately began to buckle under the weight of the vehicle.

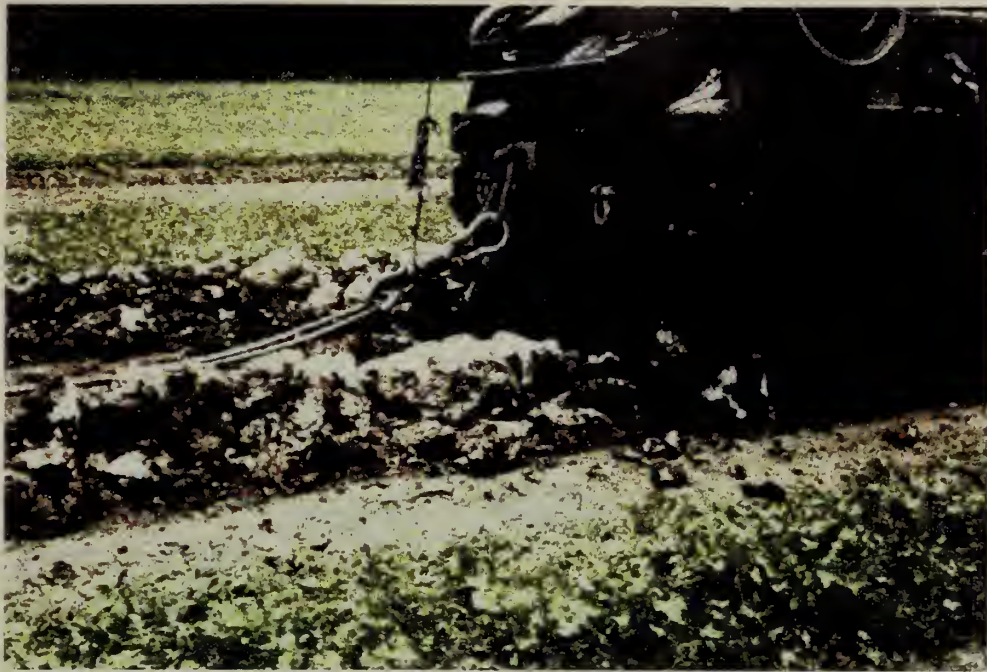


Figure 13. Foam damage during traction tests. This lower density foam did not provide additional traction for the M88A2.

The foam employed for the HMMWV traction tests had the same consistency as that for the M88A2 tests. The results of the drawbar pull tests indicate that the foam provided additional traction for the HMMWV that was towing the disabled water truck.

4. Effects on Sub-surface laid Mines

a. Set-up

Eight M15 training mines and eight pressure cells were employed under the same roadway used for the trafficability tests. Four of the pressure cells were rated at 50 psi and used for the HMMWV lane while the remaining four cells were rated at 100 psi and used for the M88A2 lane. The mines were buried approximately 2 inches deep and were set to be tripped after experiencing a load of 14 psi. The pressure cells were buried approximately 3 inches in depth and placed adjacent to the M15 mines in order to provide the loading data for each pass of a vehicle. Figure 3 shows the actual layout of each mine

and pressure cell. The data for this experiment was taken concurrently with the trafficability data.

b. Experiments

Load sensor data was taken for each of the 50 passes of the M88A2 and HMMWV.

c. Results

Without the use of the foam, the M88 was calculated to have a surface contact pressure of 17.4 psi while the HMMWV had a contact pressure of 20 psi for the front tires and 26 psi for the rear tires. The load sensors indicated an average load of 5.4 psi for the M88A2 and 0.34 psi for the HMMWV. The Phase I report by SNL calculated similar values, 5.0 psi for the M88A2 and 0.5 psi for the HMMWV [Ref. 11:p. 109]. None of the simulated mines were triggered by any of the 100 passes over the foam roadway.

C. EXPLOSIVE EXPERIMENTS

All explosive experiments were conducted at the Energetic Materials Research and Testing Center (EMRTC), Socorro, NM.

1. Explosive Effects on RPF

a. Set-up

Figure 14 shows the experimental set-up for the explosive experiments conducted at EMRTC, Socorro, NM. A twelve-inch thick layer of fine sand was placed on top of solid ground. Sand was chosen in order to provide a level surface for the foam blocks. Sand bags were placed on top of the foam blocks to ensure that the foam remained on top of the sand during the explosion. The smaller foam blocks will tend to elevate, thus causing a considerable air gap during the propagation of the explosive shock.

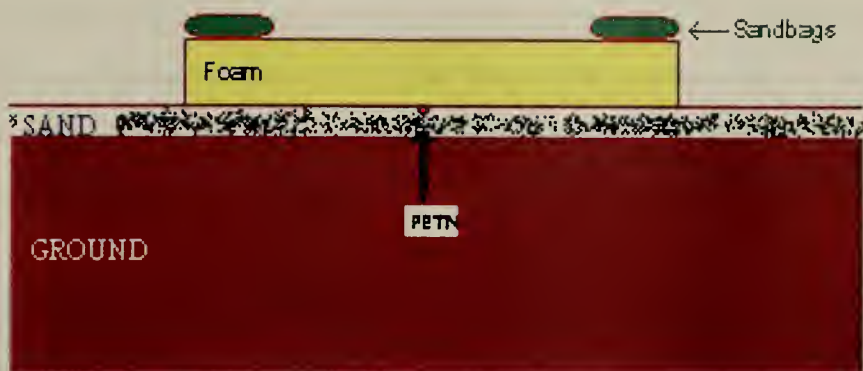


Figure 14. Schematic for Land Experiments. The sandbags are placed on the foam block in order to ensure that the foam remains on top of the sand during the explosion.



Figure 15. Ground set-up for experiments.

The explosive used for these experiments was PETN, pentaerythritol tetranitrate, which is commonly used in grenades, small caliber projectiles, and demolition

devices [Ref. 3:p. 6.13]. PETN has a conversion factor of 1.45 when scaled to TNT, i.e. 10 g PETN has the explosive effect of 14.5 g TNT. Figure 16 shows how PETN was molded to approximate the shape of a typical blast anti-personnel mine. A patty-shaped explosive was chosen over a spherical shape in order to closely replicate the explosive geometry in an anti-personnel mine.



Figure 16. PETN explosives used in experiments. The mine on the top of the figure is a VS-MK2 training AP pressure mine. The 10 g PETN were formed like the charge on the bottom left while the 30-g charge looks like the patty-shaped figure on the bottom right.

The foam blocks were poured in two different frames, 65 X 65 X 24 and 85 X 85 X 24 inches. Figure 17 shows the set-up of one frame. The frames were lined with plastic to prevent the foam from sticking to the wood. Handles were constructed to provide easy handling of the foam block after sufficient hardening.



Figure 17. Frame used to mold foam blocks. The plastic was used in order to prevent the foam from adhering to the wooden frame. The handles were used to extract the foam block from the frame.

A two-part polyurethane dispensing machine made by Decker Industries, Florida, was used to make the 15 foam blocks for this experiment. This was also the same machine used to create the foam roadway for the trafficability experiments. The machine was dispensing $3.5\text{--}4.0\text{ lb/ft}^3$ foam at an average rate of 55 lb/min . Cream time, which is the amount of time elapsed before the mixture reached a cream-like consistency, took place after 55-65 seconds. The foam reached its maximum expansion after a rise time of 3-4 minutes. Figure 18 shows the Decker foam machine used for these experiments.



Figure 18. Decker Foam Machine. The resin and isocyanate are in separate barrels located directly behind the machines control panel. The two parts are mixed in the dispensing gun just before the mixture is sprayed out of the gun.

Table 1. Matrix for Explosive Cavity Formation Experiments

| TEST I Expt # | Medium | | Block Size | Charge Size | | | Charge Depth | |
|------------------|--------|-----|------------|-------------|----|----|--------------|---|
| | Land | Sea | (cu. in) | 10 | 30 | 50 | 0 | 2 |
| L1 | X | | 65X65X6 | X | | | X | |
| L2 | X | | 65X65X6 | | X | | X | |
| L3 | X | | 85X85X6 | X | | | X | |
| L4 | X | | 85X85X6 | | X | | X | |
| L5 | X | | 65X65X12 | X | | | X | |
| L6 | X | | 65X65X12 | | X | | X | |
| L7 | X | | 85X85X12 | X | | | X | |
| L8 | X | | 85X85X12 | | X | | X | |
| L9 | X | | 65X65X18 | X | | | X | |
| L10 | X | | 65X65X18 | | X | | X | |
| L11 | X | | 85X85X18 | X | | | X | |
| L12 | X | | 85X85X18 | | X | | X | |
| MOD1 | X | | 85X85X30 | | X | | X | |
| L13 | X | | 85X85X30 | | X | | X | |
| L14 | X | | 85X85X18 | | | X | X | |
| L15 | X | | 85X85X30 | | | X | X | |

b. Experiment

Table 2 is the matrix used for the explosive cavity formation experiments.

Two different block sizes, 65" X 65" and 85" X 85", were used in order to investigate edge effects. The PETN explosive was positioned directly underneath the geometric center of each foam block. The top of the explosive was made flush with the sand surface in order maintain direct contact with the block. Nonel Primadet chord, a non-electric blasting device, was used to detonate the charge. The chord made contact with the bottom of the PETN and was routed underneath the sand towards the triggering mechanism. After each shot, measurements were taken of the ground crater, entrance cavity, exit cavity, and depth of penetration in the foam. Figure 19 and 20 show the set-up for Experiment L1.



Figure 19. PETN set-up for explosive cavity experiments. Note that the PETN is shaped to simulate an anti-personnel mine.



Figure 20. Set-up of Experiment L1. The sand bags kept the foam pad in contact with the ground during the blast. The grid in the background has an interline spacing of 1 foot.

Experiments L4 and L12 were conducted with a 3,000 pound metal plate, 72 X 72 X 2 inches placed directly on top of the foam. This metal plate simulated an external static load, such as a vehicle directly on top of a mine. The concept was to determine if damping would enhance the performance of the foam against an exploding anti-personnel mine.

c. Results

Table 2 shows the cavity diameter from all fifteen experiments. The 30-gram explosive perforated through all but the thickest foam block, MOD 1, and the 10-gram explosive was contained by foam blocks thicker than 12 inches, L5, L9, and L11. L5, 18 inches thick, which was loaded with the metal plate, was able to contain the 30-gram charge. MOD 1 was an addition to the initial matrix. It was the thickest foam block, 30 inches, and the only block without additional damping to contain the 30-gram charge.

Figures 21 ,22, and 23 show the effects of a 10-gram charge on a 6 inch block of foam. The explosive created an exit cavity (top) almost twice the size as the entry cavity (bottom) and a ground crater 21 inches in diameter. The failure of the foam block was contained to the cavity, and there were no cracks observed laterally to either side of the foam. Two modes of failure were observed on the blocks that were perforated. The direct blast failure results in the crushing of the foam cells near the entry point of the explosive while the foam's mechanical failure results in a shear plug. The shear plug creates an exit cavity significantly larger than the entry cavity. Figure 21 shows a generic sketch of the explosive effects on an RPF block.

Table 2. Results from Explosive Cavity Experiments.

| EXPT # | L X W (inches) | Thickness (inches) | Charge (grams) | Cavity Diameter | | | Depth (inches) | |
|-----------|-------------------|-----------------------|-------------------|-------------------|------------------|-------|-------------------|-------|
| | | | | Entry (inches) | Exit (inches) | | | |
| L1 | 65 X 65 | 6.00 | 10.00 | 5.75 | 11.00 | 6.00 | | * |
| L5 | 65 X 65 | 12.00 | 10.00 | 8.50 | 0.00 | 7.00 | | |
| L9 | 65 X 65 | 18.00 | 10.00 | 6.00 | 0.00 | 6.00 | | |
| L2 | 65 X 65 | 6.00 | 30.00 | 8.50 | 18.50 | 6.00 | | * |
| L6 | 65 X 65 | 12.00 | 30.00 | 11.50 | 18.25 | 12.00 | | * |
| L10 | 65 X 65 | 18.00 | 30.00 | 9.75 | 15.50 | 18.00 | | * |
| L3 | 85 X 85 | 6.00 | 10.00 | 4.75 | 13.75 | 6.00 | | * |
| L7 | 85 X 85 | 12.00 | 10.00 | 4.50 | 10.25 | 12.00 | | * |
| L11 | 85 X 85 | 18.00 | 10.00 | 5.75 | 0.00 | 6.50 | | |
| L4 | 85 X 85 | 6.00 | 30.00 | 8.25 | 14.25 | 6.00 | | *, ** |
| L8 | 85 X 85 | 12.00 | 30.00 | 7.75 | 19.25 | 12.00 | | * |
| L12 | 85 X 85 | 18.00 | 30.00 | 8.50 | 12.50 | 18.00 | | *, ** |
| L13 | 85 X 85 | 18.00 | 30.00 | 11.20 | 0.00 | 11.20 | | |
| Mod 1 | 85 X 85 | 30.00 | 30.00 | 5.75 | 0.00 | 11.85 | | |
| L14 | 85 X 85 | 18.00 | 50.00 | 7.20 | 10.80 | 18.00 | | |
| L15 | 85 X 85 | 30.00 | 50.00 | 10.70 | 0.00 | 12.80 | | |
| * failure | | | | | | | | |
| ** loaded | | | | | | | | |

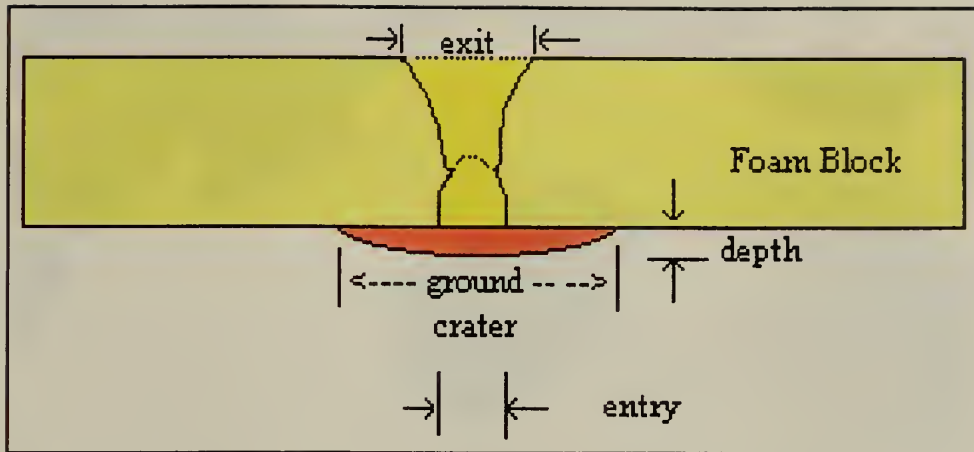


Figure 21. Sketch of the explosive effects on an RPF block. Note that the ground crater is significantly larger than both entry and exit craters. This is a sketch of the cross section of foam block L10, 18" thick, 30-gram PETN charge (not drawn to scale). L10 was perforated by the explosive. The bottom section of the foam cavity (dark yellow) is the result of the direct blast while the upper portion (shear plug) results from mechanical failure.

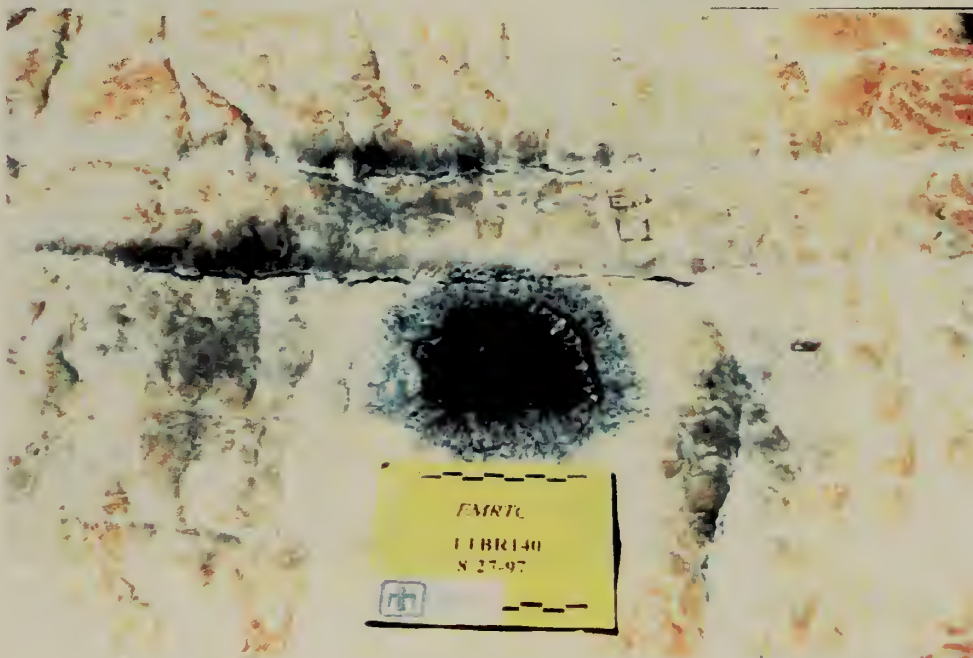


Figure 22. Entry cavity for Experiment L1, 6" thick, 10-gram charge.

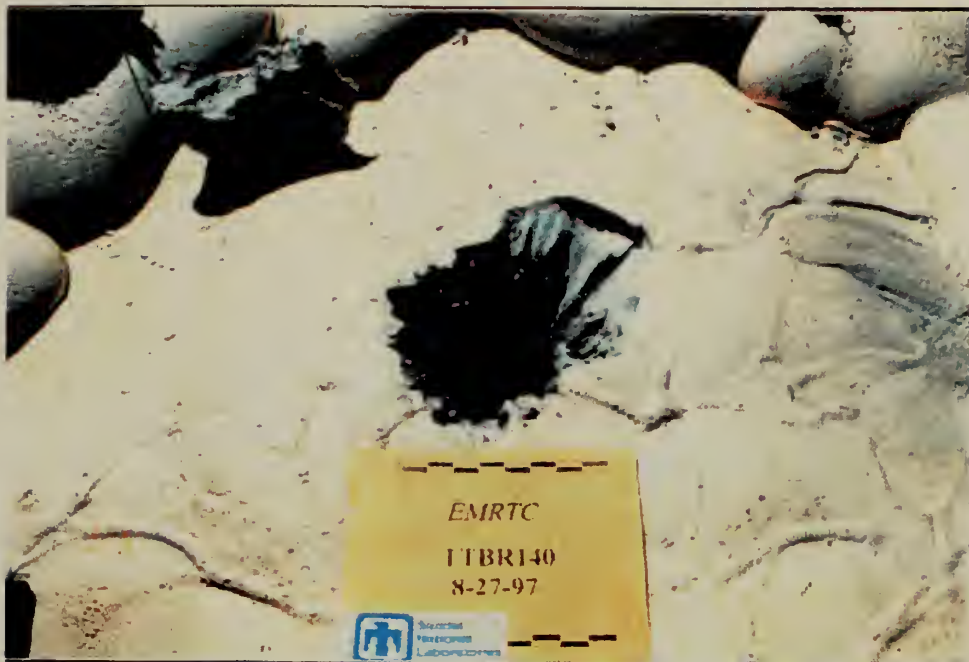


Figure 23. Exit cavity for Experiment L1, 6" thick, 10-gram charge

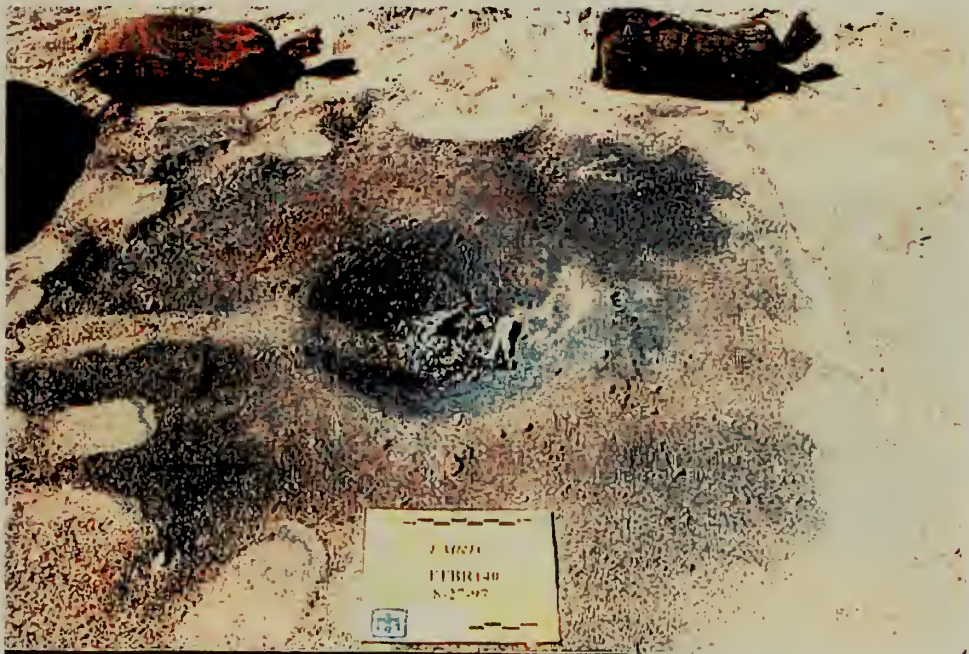


Figure 24. Ground crater from Experiment L1, 6" thick, 10-gram charge.

Figure 25, 26 and 27 show the results of a 10 gram PETN charge on an 18-inch thick foam block, L9. L9 completely contained the effects of the 10 gram charge. The entry cavity diameter and the depth of penetration were both 6 inches. The top

surface (exit) of the foam block had no cracks or fissures. The ground crater was measured to be 18.5 inches in diameter and 2.9 inches deep.



Figure 25. Entry Cavity for Experiment L9, 18 " thick, 10-gram charge.



Figure 26. Exit Cavity for Experiment L9 (No perforation), 18 " thick, 10-gram charge.

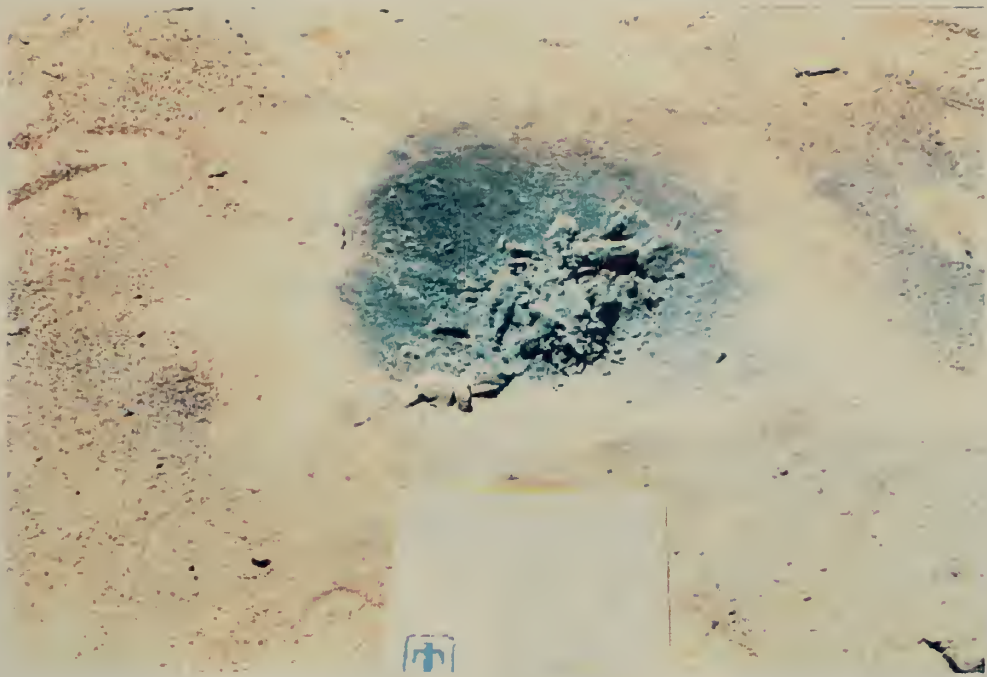


Figure 27. Ground Crater from Experiment L9, 18 " thick, 10-gram charge.

2. Repair of Damaged RPF Blocks

a. Set-up

The damaged foam blocks used for these experiments were the blocks used for the cavity formation experiments. The damaged blocks were placed on a flat surface with the exit cavities facing up. Figure 27 shows the initial set-up for the repair experiments.

b. Experiments

These experiments were conducted to determine the most efficient method of repairing a damaged foam block and its subsequent strength. Figures 28, 29, and 30 show how the damaged foam was repaired. By pouring the foam directly into the damaged cavity, some of the foam escaped through the bottom. Once the foam began to rise, it quickly adhered to the interior of the block.

c. Results

Figure 29 shows a cross-section of the repaired foam block. It is evident that the foam not only filled the cavity, but it also seeped through the smaller cracks in the interior wall. Cold joints were formed at the boundary between the new and old joints. Follow-on experiments will determine the resulting strength of these repaired foam blocks. Figure 31 shows a schematic of a repaired foam block.

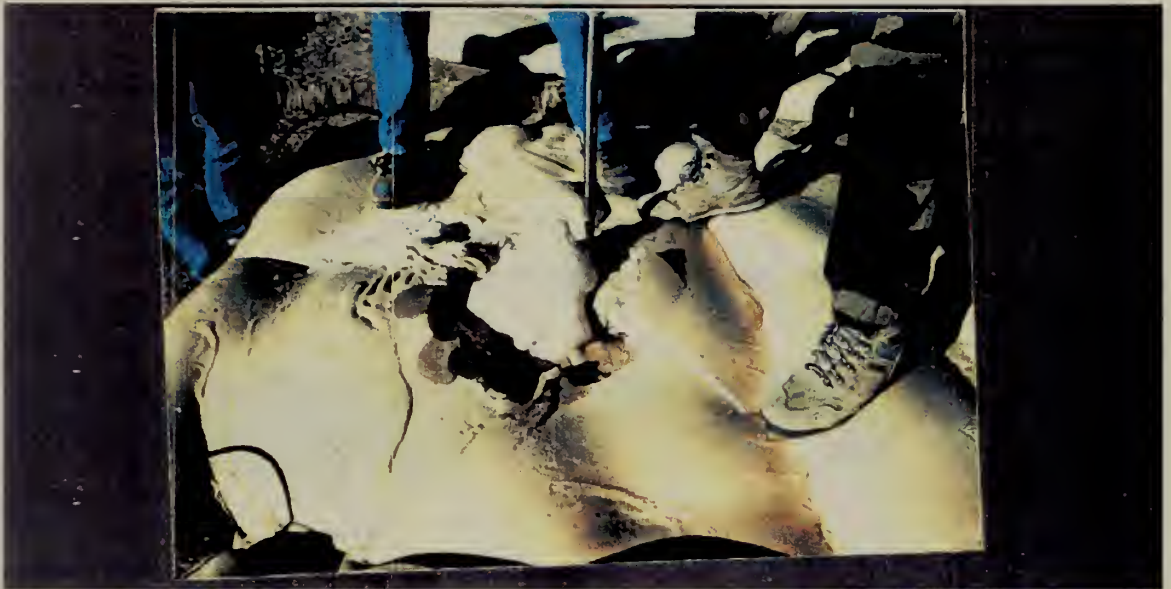


Figure 28. Dispensing Foam into damaged section



Figure 29. Top surface of a repaired block of foam

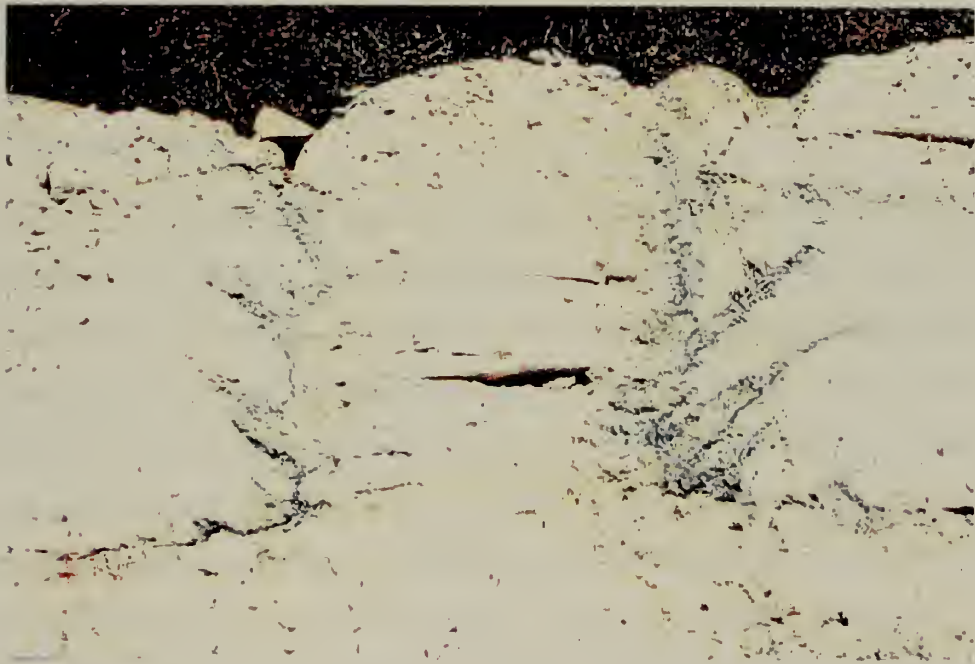


Figure 30. Cross section of repaired block of foam. Notice the cold joints that are formed between the new and original foam.

IV. ANALYSES

A. WATERWAYS EXPERIMENTS

1. Trafficability

These trafficability experiments were conducted to determine if RPF, at a given thickness and density, can provide a durable lane for multiple passes of track and wheel vehicles. The 24-inch thick, 4 lb/ft³ roadway successfully withstood 50 passes of the M88A2 and HMMWV with a maximum rut depth of 3 inches throughout the length of the roadway. An M1A1 tank battalion consists of four tank companies. The battalion would have a total of 58 M1A1 tanks, 10 M88A2 Recovery vehicles, and an assortment of trucks, and Armored Personnel Carriers (APC). The M88A2 is the heaviest vehicle in the unit and it would inflict the most damage to the foam roadway. The minimal damage created by 50 passes of the M88A2 would suggest that the foam roadway will be able to carry the passage of at least an entire battalion before repairs would have to be made on the foam.

2. Traction Tests

Results of the drawbar-pull experiments indicate that the foam did not increase the pulling capability of the M88A2. Instead, the foam decreased the traction of the M88A2 by 7 percent of the vehicle weight. On the other hand, the HMMWV's pulling capability was increased by 20 percent of the vehicle weight [Ref. 6:p. v]. It was observed that when the foam was dispensed on the watered down rut, the foam expanded into a less dense and porous material. Even several hours after the experiments were conducted, the foam retained its spongy consistency. The amount of foam poured into the water logged ruts of the M88A2 was only 3 - 5 inches in depth. Since a lower foam density was predicted because of the presence of water, more foam should have been poured for the M88A2 experiments. Additional experiments will have to be conducted in order to determine the amount of foam needed to increase the drawbar-pull capability of the M88A2 by more than 10 percent of its weight in poor conditions [Ref. 6:p. 36].

Figure 31 shows the initial drawbar-pull coefficient, slip percentage, and work index from the M88A2 test on dry surface [Ref. 6:p. 14]. The optimum drawbar-pull coefficient of 0.69 occurs at a slip of 22%. This slip percentage is taken at the maximum work index of 0.55. The drawbar-pull coefficient is a measurement of the load being pulled by the lead vehicle with respect to a certain slip condition. The coefficient is obtained by normalizing the load to the weight of the vehicle. The work index for each slip value is calculated by multiplying the load by the distance represented by $1 - \text{slip \%}$.

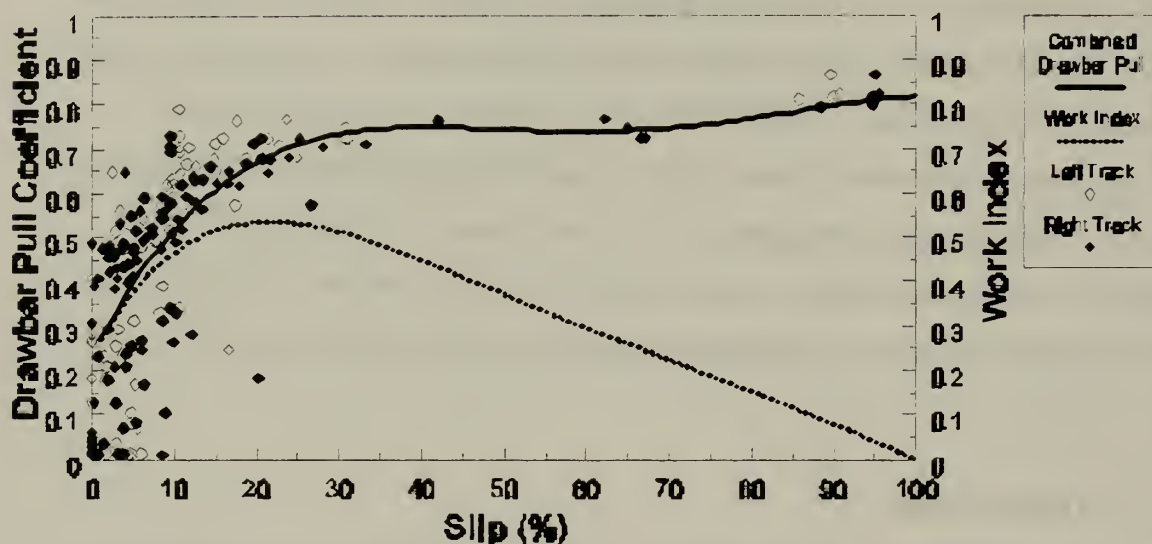


Figure 31. From Ref. [6], Dry Surface drawbar-pull test on M88A2

When the track ruts were filled in with 1-2 inches of water, the M88A2 recorded a decrease in the drawbar-pull coefficient from 0.69 to 0.20. The work index decreased from 0.55 to 0.15. Figure 32 shows these parameters for the wet surface, drawbar-pull tests for the M88A2 [Ref. 6:p. 15]. It is also evident from the data that there was no significant difference in the left and right track.

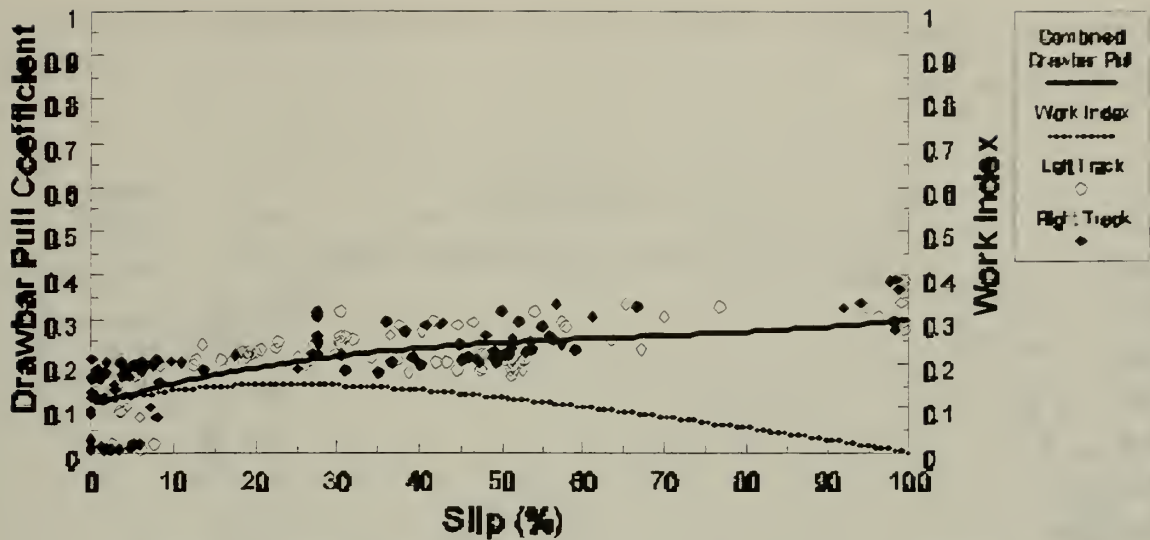


Figure 32. From Ref. [5], Wet surface drawbar-pull test on M88A2.

After the foam was dispensed into the wet track rut, the optimum drawbar-pull coefficient decreased to 0.14 at 22 percent slip. The maximum work index was 0.1. Figure 33 shows the results of the experiments on the foam-filled ruts [Ref. 6:p. 15].

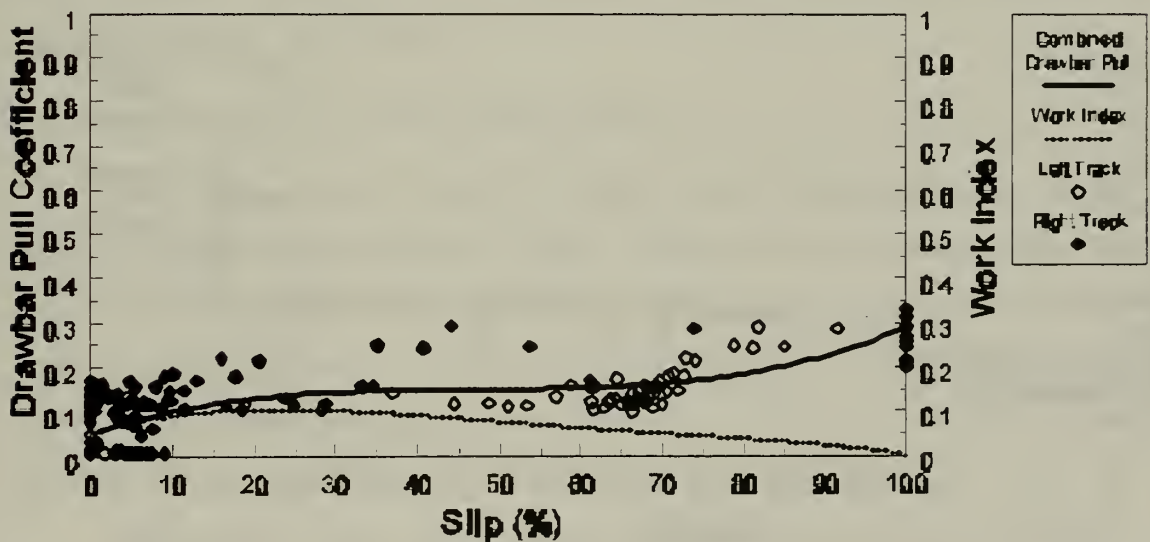


Figure 33. From Ref. [5], Foam surface drawbar-pull test on M88A2

Figures 34, 35, and 36 show the corresponding output for the HMMWV experiments [Ref. 6:p.16-17]. On dry surface, the optimum drawbar-pull coefficient was 0.75 at a slip of 25 percent. The drawbar-pull coefficient decreased to 0.30 at 30 percent

slip during wet surface tests, but increased to 0.50 at 33 percent slip when the HMMWV was tested on the foam.

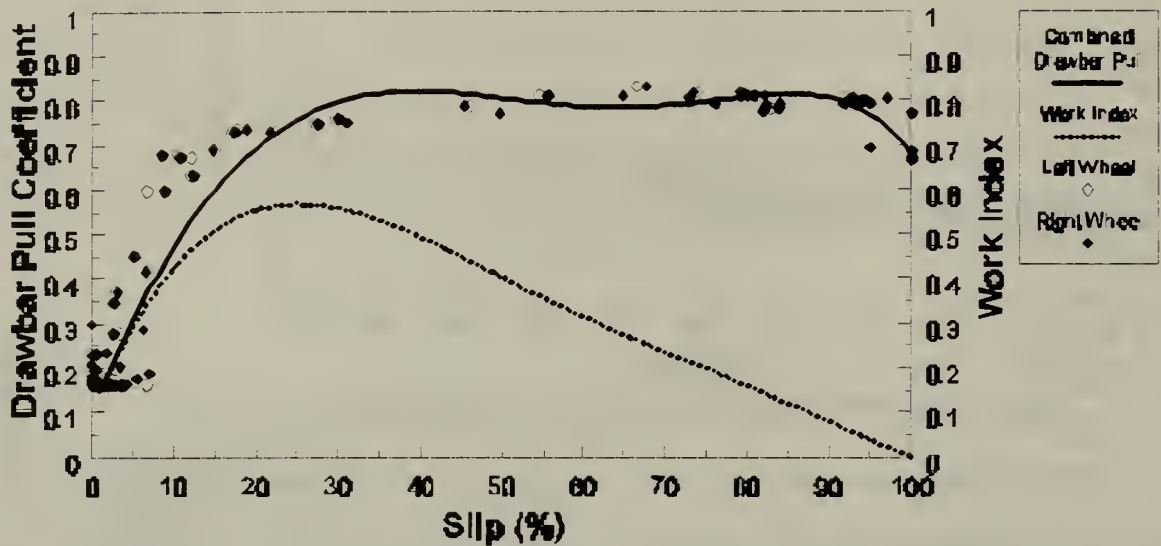


Figure 34. From Ref. [5], Dry Surface drawbar-pull test on HMMWV

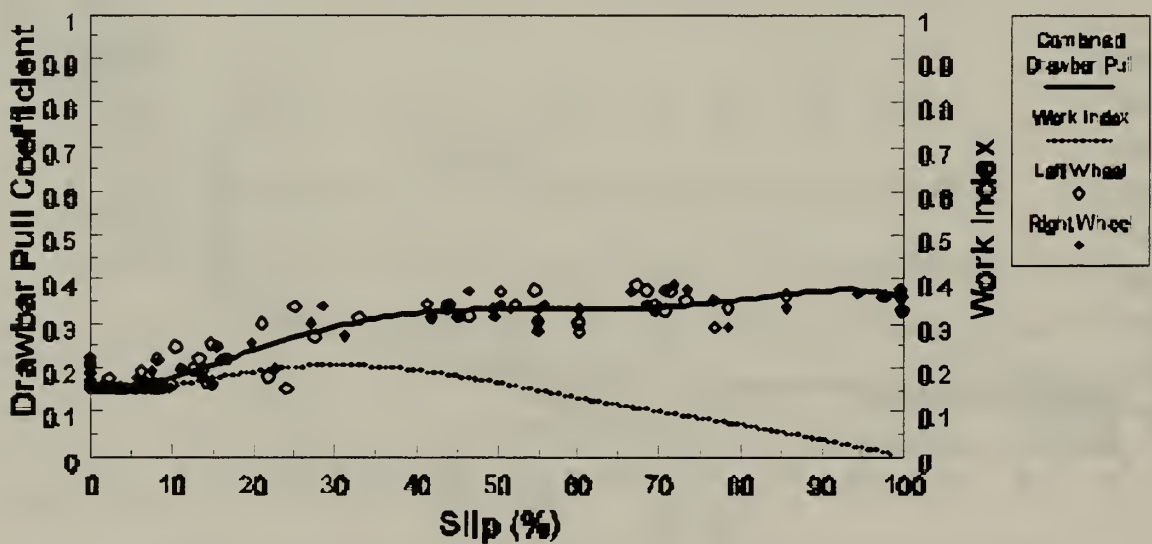


Figure 35. From Ref. [5], Wet Surface drawbar-pull test on HMMWV

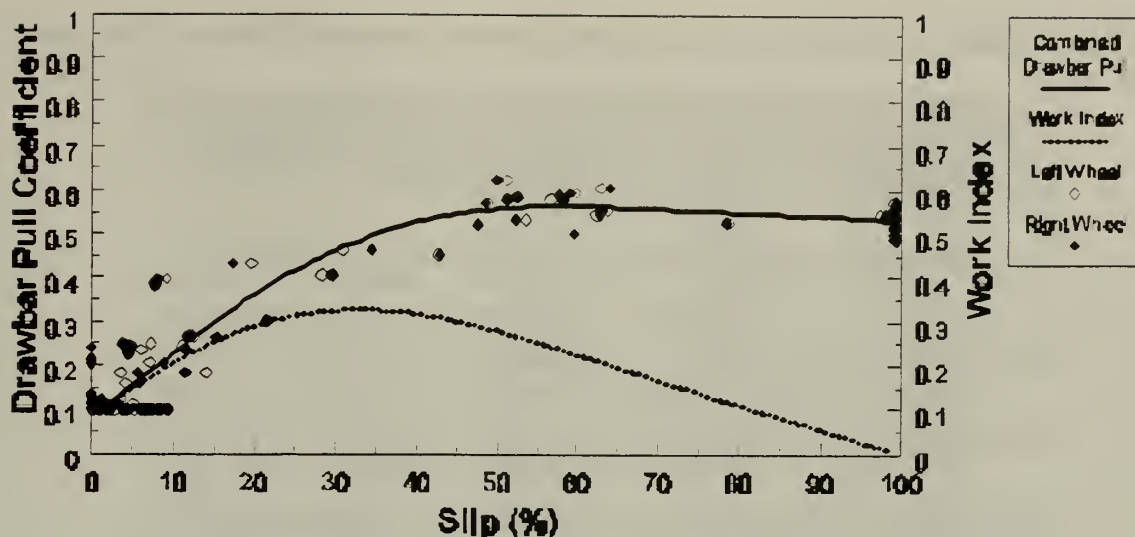


Figure 36. From Ref. [5], Foam Surface drawbar-pull test on HMMWV.

The decrease in traction for the M88A2 can be attributed to the less dense foam that resulted from the mixture of water with the resin and isocyanate. Unlike the M88A2 which completely destroyed the foam in the rut, the HMMWV merely crushed the top layer of the foam. Despite the lower density foam, the intact foam provided a 66 percent increase in drawbar-pull coefficient.

3. Foam Effects on Subsurface laid Mines

The average pressure exerted by the M88A2 on the foam roadway was 5.40 psi while the HMMWV had an average of 0.34 psi. Table 3 shows a summary of the effects of a 24 inch foam roadway on selected anti-tank mines. Only 2 of the 13 anti-tank mines would be activated by the load of a dynamic load of a M88A2. The HMMWV would not activate any of these anti-tank mines under similar test conditions. Even for the activated mines, the foam should mitigate the blast effects of the anti-tank mines.

Tables 4 and 5 [Ref. 6: p 9] lists some typical pressure and trip-wire fused anti-personnel mines and their corresponding activation pressures. If these mines were encapsulated by RPF under similar test conditions, the M88A2 would activate 7 of the 8 anti-personnel pressure fused mines. The HMMWV would not activate any of the listed mines. These measurements imply that foot traffic would not activate any of these anti-personnel mines.

Table 3. Summary of anti-tank mines neutralized due to 60 cm application of foam, After Ref. [5].

| <i>Mine Type</i> | <i>Origin</i> | <i>Activation Pressure</i> | <i>M88A2 Activated</i> | <i>HMMWV Activated</i> |
|------------------|------------------|----------------------------|------------------------|------------------------|
| MK-7 | UK | 4.21 | * | |
| SH-5TC-65 | Italian | 5.19 | * | |
| TM-46 | Italian/Egyptian | 10.31 | | |
| TM-57 | Russian | 6.24 | | |
| TM-62 | Russian | 6.93 | | |
| VS-2.2 | Russian | 11.59 | | |
| TC/2.4 | Italian/Egyptian | 10.31 | | |
| SBB/81 | Italian | 8.59 | | |
| VS-1.6 | Italian | 10.88 | | |
| M15 | US | 7.92 | | |
| M19 | US | 6 | | |
| M21 | US | 5.77 | | |

* Based on average pressure

Average M88A2 Pressure @ 50 passes = 5.40 psi

Maximum M88A2 Pressure @ 50 passes = 7.0 psi

Average HMMWV Pressure @ 50 passes = 0.34 psi

Maximum HMMWV Pressure @ 50 passes = 0.54 psi

Table 4. Effects of M88A2 and HMMWV on Anti-personnel (Pressure Fuzed) mines, After Ref. [5].

| <i>Mine Type</i> | <i>Origin</i> | <i>Fuse Type</i> | <i>Activation Pressure</i> | <i>M88A2 Activated</i> | <i>HMMWV Activated</i> |
|------------------|---------------|------------------|----------------------------|------------------------|------------------------|
| | | | (psi) | | |
| PMN | Russian | Pressure | 0.92 | * | |
| PMN-02 | Russian | Pressure | 0.58 | * | |
| PMD-6 | Russian | Pressure | 0.47 | * | |
| VAL 69 | Italian | Pressure | 1.08 | * | |
| SB-33 | Italian | Pressure | 7.7 | | |
| VS-MK2 | Italian | Pressure | 2.29 | * | |
| PFM-1 | Russian | Pressure | 2.24 | * | |
| M14 | US | Pressure | 2.86 | * | |

Table 5. Effects of M88A2 and HMMWV on Anti-personnel (Tripwire Fuzed) mines, After Ref. [5].

| <i>Mine Type</i> | <i>Origin</i> | <i>Fuse Type</i> | <i>Activation Pressure</i> | <i>M88A2 Activated</i> | <i>HMMWV Activated</i> |
|------------------|---------------|------------------|----------------------------|------------------------|------------------------|
| | | | (psi) | | |
| POMZ-2 | Russian | Trip-wire | 7 | | |
| MON-50 | Russian | Trip-wire | 7 | | |
| MON-100 | Russian | Trip-wire | 7 | | |
| MON-200 | Russian | Trip-wire | 7 | | |
| OZM-3 | Russian | Trip-wire | 7 | | |
| OZM-4 | Russian | Trip-wire | 7 | | |
| OZM-72 | Russian | Trip-wire | 7 | | |
| P-40 | Italian | Trip-wire | 11 | | |
| VAL 69 | Italian | Trip-wire | 13.2 | | |
| M16A1 | US | Trip-wire | 6.5 | | |
| M1 Fuse | US | Trip-wire | 4 | | |
| M1A1 Fuse | US | Trip-wire | 10 | | |
| M3 | US | Trip-wire | 6 | | |

Waterways Experiment Station plotted the maximum pressure of each vehicle pass for the M88A2, Figure 37 [Ref. 6:p. 10]. The graph indicates that the vehicle exerted higher pressures when the passes were conducted in the reverse direction as opposed to the forward direction. The M88A2 's maximum pressure was 7 psi on the second reverse pass and a minimum of 3 psi on the fourth forward pass. After the 44th pass, the pressures for both directions converge to about 6 psi. These numbers suggest that as the rut became deeper, the foam became stronger. As the debris in the rut became compacted, the crushed layer efficiently cushioned the impact of the vehicles [Ref. 6: p 9-10].

Figure 37 also shows that the M88A2 recorded higher pressures in the reverse direction. This can be explained by the manner in which the track advances in the reverse direction. In the reverse direction, the track exerts its maximum load directly underneath the final roadwheel. In the forward direction, track bridging takes place. This allows the weight to be distributed over a larger piece of track.

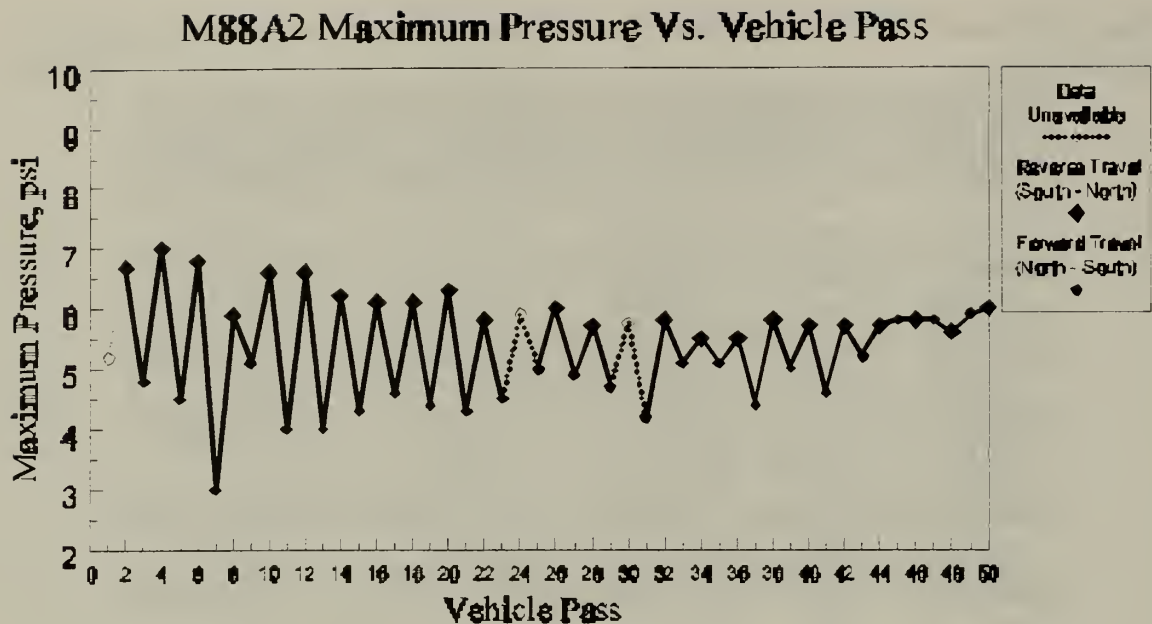


Figure 37. Change in maximum pressure versus pass number, After Ref. [5]

4. Foam Effects on Trip Wire

All of the trip wire devices placed in the proposed foam roadway were tripped by the expansion of the foam. The activation of trip-wire detonated mines within or adjacent to the roadway further decreases the threat posed to vehicular and foot traffic.

B. EXPLOSIVE EXPERIMENTS

1. Explosive Cavity Formations in RPF.

Based on the experimental results taken by Cooper and Kurowski, and Woodfin [Ref 12:p.43], predictions were made of the cavity sizes resulting from 10, 30, and 50 gram PETN explosives. Table 6 presents measured cavity diameters compared to the predictions based on earlier work.

Table 6. Predicted and Actual Cavity Results for 4 lb/ft³ foam

| Cavity (inches) | Explosive Charge PETN (Grams) | | |
|----------------------------|--|-------|-------|
| | 10 | 30 | 50 |
| Predicted | 12.00 | 17.00 | 19.00 |
| Actual | 5.30 | 10.00 | 10.70 |

The earlier works were based on C-4 and the present measurements were made with PETN. The experiments conducted by Cooper and Kurowski, and by Woodfin used C-4 as the explosive charge. C-4 has a TNT equivalent of 1.30 while PETN has an equivalent of 1.45 [Ref. 3:p. 76]. These results indicate that explosive charges placed between the ground and a foam block interface resulted in cavities which were smaller than the cavities formed from surface and embedded shots. The difference in cavity diameters for the three charges are 56%, 41%, and 47% for 10, 30, and 50 grams respectively.

Figure 38 shows the predicted plot for the 4 lb/ft³ foam (blue). The 2 lb/ft³ and 14 lb/ft³ foam are depicted in red and green respectively. The experimental matrix for the PETN shots were based on the surface and embedded empirical data.

Figure 39 shows how the cavity data from the ground shots compares with the surface and embedded shots. The blast cavity diameters created by the ground shots were significantly smaller than the surface and embedded shots. The present experiment suggests that when the explosive lies between the ground and foam pad, more energy is absorbed by the ground, lessening the impact on the foam. Additionally, the ground shots exhibit the same charge scaling as the surface and embedded shots.

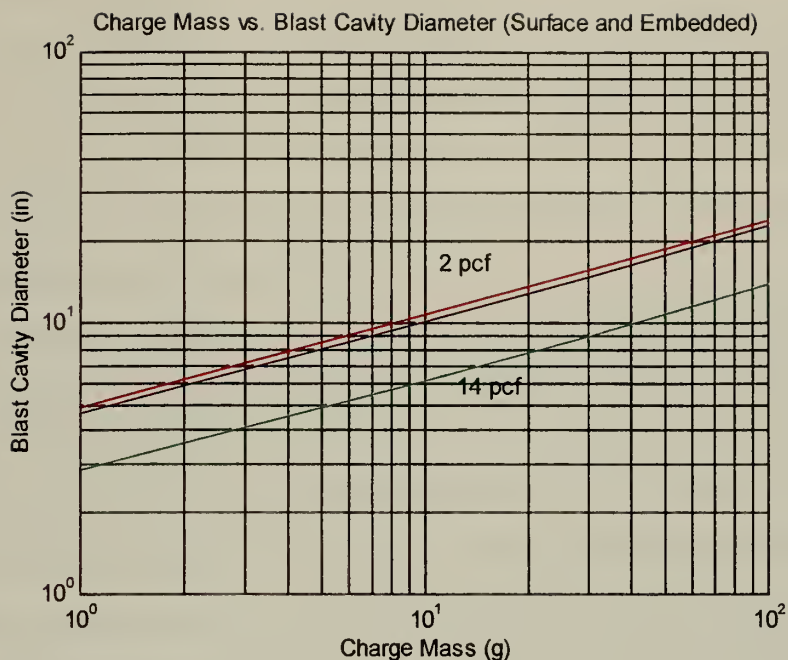


Figure 38. Cavity Prediction for 4 lb/ft³ based on Surface and Embedded Data (C-4). The red and green lines depict the 2 lb/ft³ and 14 lb/ft³ Surface and Embedded data respectively.

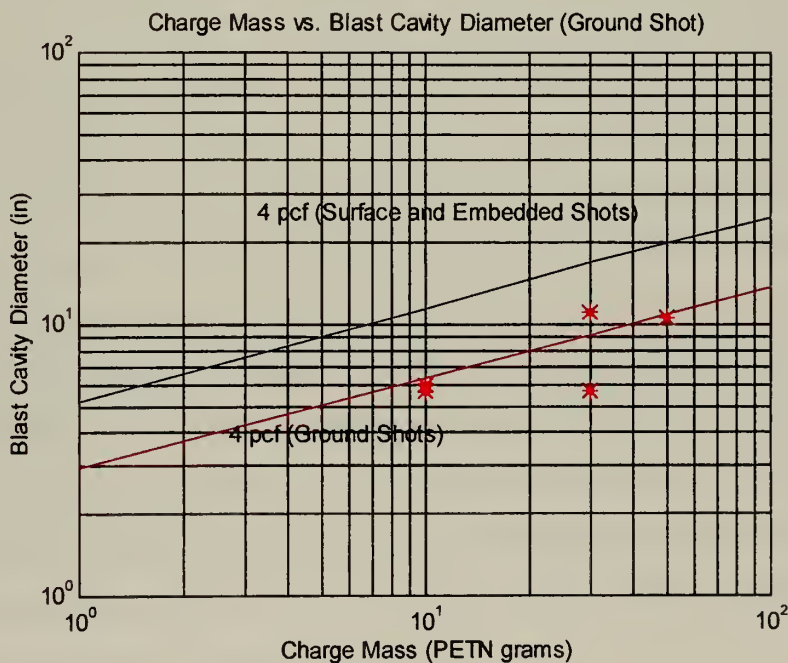


Figure 39. Comparison between Ground Shots and Surface and Embedded Shots. Note that the ground shots created smaller cavity diameters.

Table 7 shows a comparison of the cavity results for the two different block sizes to investigate the effect of edges. The data shows that the cavity sizes are very similar regardless of whether the foam block contained the explosive blast or was perforated by the blast. The 10 gram charge showed a 10% difference in cavity size while the 30 gram charge showed a 16% difference between the two different thickness. These numbers indicate that edge effects were not significant.

Table 7 also shows an approximate threshold charge before perforation occurs. The 10 gram charge can be completely contained by a block thickness of 18 inches while the 30 gram can be contained by a 30-inch block. A 50 gram charge was also completely contained by a 30-inch block. Additional experiments have to be conducted in order to determine a more precise failure criteria for a given charge and foam block thickness. Table 6 provides a graphical means to predict the cavity depth created by larger yields. Figures 39 and 40 are generated by using cube-root scaling on the measured cavity depth and cavity diameters. Using the cube-root scaling equation,

$$D = AW^{1/3}, \quad (1)$$

where D is the cavity depth in inches, A is a constant with units $\text{in/g}^{1/3}$, and W is the yield in grams, we can calculate the constant, A, in order to predict cavity depths from larger yields. For the 4 lb/ft³ foam, A has a value of 3.26 $\text{in/g}^{1/3}$. This constant yields the cavity depth and cavity diameter predictions in Table 8. Using these predictions for the 4 lb/ft³ foam, a VS - 1.6 anti-tank mine, which has 1.7 kg of TNT, would create a 31-inch cavity diameter with a cavity depth of 35 inches. Similarly, the M19 anti-tank mine, which has 9.5 kg of Comp B, would create a 61-inch cavity diameter with a cavity depth of 67 inches. These numbers suggest that in order to completely contain an anti-tank mine similar to the M19, the foam roadway would have to be much larger than 67 inches thick. Additional experiments will have to be conducted in order to obtain a foam density that can provide an operationally capable foam roadway.

Table 7. Comparison of Cavity Diameters and possible Edge Effects.

| EXPT # | L X W (inches) | Thickness (inches) | Charge (grams) | Cavity | | Diameter Depth | |
|--------|-------------------|-----------------------|-------------------|-------------------|------------------|-------------------|-------|
| | | | | Entry (inches) | Exit (inches) | | |
| L1 | 65 X 65 | 6 | 10 | 5.75 | 11.00 | 6.00 | * |
| L3 | 85 X 85 | 6 | 10 | 4.75 | 13.75 | 6.00 | * |
| L5 | 65 X 65 | 12 | 10 | 8.50 | 0.00 | 7.00 | |
| L7 | 85 X 85 | 12 | 10 | 4.50 | 10.25 | 12.00 | * |
| L9 | 65 X 65 | 18 | 10 | 6.00 | 0.00 | 6.00 | |
| L11 | 85 X 85 | 18 | 10 | 5.75 | 0.00 | 6.50 | |
| L2 | 65 X 65 | 6 | 30 | 8.50 | 18.50 | 6.00 | * |
| L4 | 85 X 85 | 6 | 30 | 8.25 | 14.25 | 6.00 | *, ** |
| L6 | 65 X 65 | 12 | 30 | 11.50 | 18.25 | 12.00 | * |
| L8 | 85 X 85 | 12 | 30 | 7.75 | 19.25 | 12.00 | * |
| L10 | 65 X 65 | 18 | 30 | 9.75 | 15.50 | 18.00 | * |
| L12 | 85 X 85 | 18 | 30 | 8.50 | 12.50 | 18.00 | ** |
| L13 | 85 X 85 | 18 | 30 | 11.20 | 0.00 | 11.20 | |
| Mod 1 | 85 X 85 | 30 | 30 | 5.75 | 0.00 | 11.85 | |
| L14 | 85 X 85 | 18 | 50 | 7.20 | 10.80 | 18.00 | * |
| L15 | 85 X 85 | 30 | 50 | 10.70 | 0.00 | 12.80 | |

* failure
** loaded

Table 8. Predicted values for Cavity Depth and Cavity Diameter for 4 lb/ft³ foam.

| Cavity (in) | Yield (grams) | | | | | |
|-------------|---------------|-------|-------|-------|-------|-------|
| | 100 | 300 | 500 | 1000 | 3000 | 5000 |
| Depth | 15.10 | 21.80 | 25.90 | 32.60 | 47.00 | 55.80 |
| Diameter | 13.70 | 19.80 | 23.50 | 29.60 | 42.70 | 50.60 |

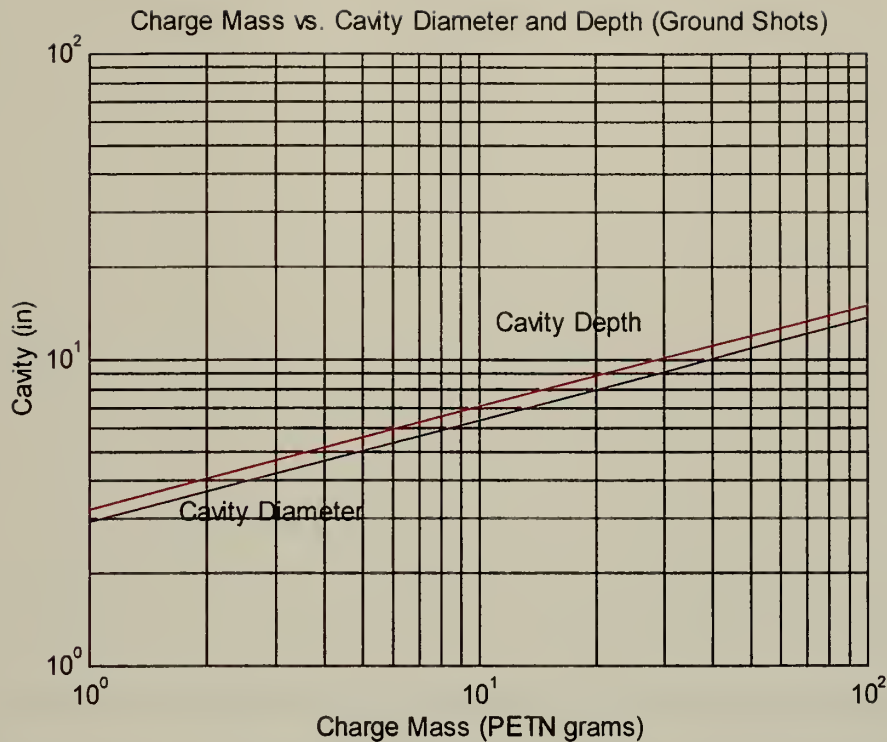


Figure 40. Charge Mass vs. Blast Cavity Diameter and Depth. Note that the cavity depth and diameters are only slightly different. This suggests that the blast cavity is semi-elliptical in shape. The red line represents the cavity depth while the blue represents the cavity diameter.

2. Repair of RPF explosive cavities.

The cavities of the damaged foam blocks were easily repaired by simply pouring foam into the damaged areas. During the foaming process, the foam would creep into all of the empty voids in the block. This process results in a repaired foam block that can be used to perform its original function, such as a roadway or an airport runway. Follow-on experiments will have to be conducted in order to compare the repaired block's initial and final properties. Figure 42 shows a sketch of the repaired foam block.

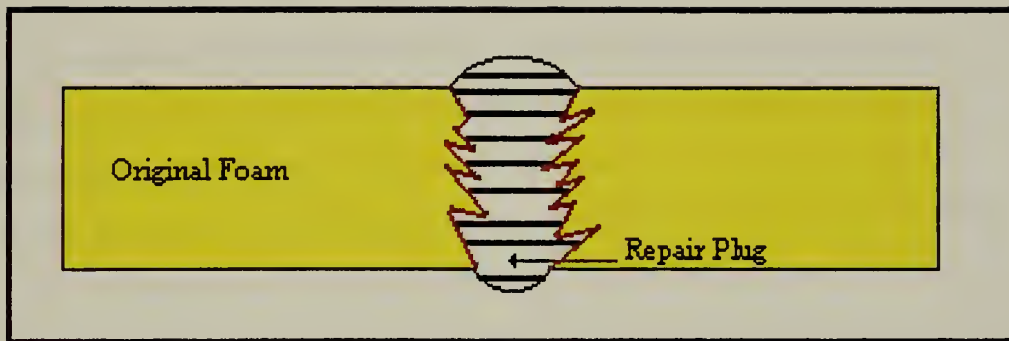


Figure 41. Sketch of a repaired foam block. Note that the new foam completely fills the cavity formed by the explosive blast. A cold joint is formed at the interface between the new and old foam.

V. CONCLUSIONS AND RECOMMENDATIONS

A. CONCLUSIONS

The test results gathered from the Waterways Experiment Station indicate that a 24-inch thick, 4 lb/ft³ Rigid Polyurethane Foam roadway adequately supported multiple passes of a track and wheeled vehicle. More importantly, the foam roadway was able to neutralize the mines buried underneath the foam and activate all trip wire detonated devices in the breach lane. Traction tests revealed that the foam did not improve traction for the M88A2 and only slightly increased the traction of the HMMWV. As for its use as a breaching technique for anti-personnel mines, the foam roadway itself serves as a very efficient breach lane, but it currently can not be employed in the timely manner needed for breaching exercises. The current dispensing machine can not dispense large enough quantities of foam in the required time for a in-stride breach.

The explosive cavity formation tests by Sandia National Laboratories indicate that a blast anti-personnel mine with 30 grams of PETN can be adequately contained by a 16-inch thick, 4 lb/ft³ foam block. A 10 gram PETN charge can be contained by a 14-inch thick, 4 lb/ft³ foam block. This thickness is reduced when the foam is statically loaded.

The combined results of the two test sites indicate that the same 24-inch thick foam roadway constructed by Waterways should be able to withstand the explosive effects of a 30-gram PETN charge. Based on cube root scaling laws, the 24-inch foam roadway should be able to completely contain a 10-gram PETN charge, and the 30-gram data suggests that the foam roadway could contain a significantly larger charge. Energy absorption experiments are currently being conducted by Sandia National Laboratories in order to determine the amount of energy that is mitigated by the foam. The amount of foam needed to contain a specific explosive can be determined from the energy absorption properties of the foam.

These feasibility experiments indicate that Rigid Polyurethane Foam, at a given density and thickness, can withstand the explosive effects of anti-personnel blast mines and mitigate or neutralize the effects of surface laid anti-tank mines.

B. RECOMMENDATIONS

1. Conduct larger scaled explosive tests in order to determine the foam's performance against anti-tank mines. These test matrix should also include different foam densities. Peter Rand, a foam specialist at Sandia National Laboratories, suggested that foam densities between 8-10 lb/ft³ would drastically increase the foam's ability to contain larger explosives.
2. Design or purchase a foam dispensing system that can dispense large volumes of foam from a considerable stand-off distance from a mine obstacle.
3. Conduct scaled explosive experiments to determine the structural effects of a mine detonated underneath an RPF block.
4. Evaluate other foam materials that may result in higher densities after water immersion.
5. Conduct experiments to determine the amount of explosive energy that is attenuated by RPF at a given density and thickness.

VI. OTHER CONSIDERATIONS AND APPLICATIONS

A. UNDERWATER EXPLOSIVE CAVITY FORMATIONS

Underwater explosive cavity formation experiments have also been conducted on RPF blocks in order to determine the effects of detonating underwater mines from varying depths. Figure 42 depicts the experimental set-up for the underwater explosive experiments. These experiments were conducted at the Energetic Materials and Research Training Center at Socorro, NM.



Figure 42. This is the set-up for the Underwater Explosive Experiments. This foam block is 6" thick and the explosive, PETN, is placed directly underneath the foam block. The PETN charge will also be located 12" and 24" underneath the foam.

B. ENERGY ABSORPTION PROPERTIES OF RPF

Experiments will be conducted by Sandia National Laboratories in November 1997 in order to determine how much energy is absorbed by an RPF foam block. These experiments will investigate the velocity of foam fragment particles impacting on a witness plate to determine how much foam will be required in order to contain the blast of a small

scale explosive. The results from these experiments will be used to predict the foam's energy absorption properties against larger explosives such as anti-tank mines. Eventually, a real anti-tank mine will be detonated underneath a tank statically loaded on an RPF foam block to investigate the structural effects on the tank.

C. LOGISTICAL CONSIDERATIONS

A variety of logistical considerations will need to be investigated in order to determine if RPF can be operationally employed on the battlefield. Currently, the foam can not be dispensed in the large quantities required for breaching operations. This technology would also have to be employed in a timely manner under all weather conditions. Since the component temperature is crucial to final outcome of the foam, the dispensing mechanism may need an intricate heating system that will keep the two components at operating temperature, especially when used in cold environments. A Stockpile to Target Sequence (STS) study will have to be conducted in order to evaluate the foam's performance in known and assumed threat environments.

LIST OF REFERENCES

1. Archulete, M. and W. Stocum, *Toxicity Evaluation and Hazard Review for Rigid Foam*, Sandia National Laboratories, 1994.
2. Bailey, A and S. Murray, *Explosives, Propellants & Pyrotechnics*, Brassey's (UK), Ltd., 1989.
3. Coppens A. and R. Reinhardt, *Explosives and Explosions*, Naval Postgraduate School, 1995.
4. Hambric, H. and W. Schneck, *The Anti-personnel Mine Threat*, Night Vision Electronic Sensors Directorate, 1994.
5. Hespe, H., *Guide to Engineering Plastic Families: Thermosetting Resins*, Mobay Corporation, 1983.
6. Mason, G. and K. Hall, *Rigid Polyurethane Foam Countermine and Traction Concept Evaluation Program*, Waterways Experiment Station, 1997.
7. North Carolina Foam Industries, *MSDS: Aromatic Isocyanate*, NCFI, 1996.
8. North Carolina Foam Industries, *MSDS: Polyol Resin System*, NCFI, 1996.
9. Rand P. and B. Hance, *Foam for Barrier Crossing: Initial Properties*, Sandia National Laboratories, 1995.
10. Rand P. and B. Hance, *Foam for Barrier Crossing: Mechanical Properties as a Function of Density, Temperature, and Time After Pour*, Sandia National Laboratories, 1995.
11. Rand P., Interview with Peter Rand on September 11, 1997, SNL.
12. Strong, B., *Plastics, Materials and Processing*, Prentice-Hall Inc., 1996.
13. Woodfin, R., *Rigid Polyurethane Foam (RPF) Technology for Countermine (Sea) Program - Phase 1*, Sandia National Laboratories, Albuquerque, NM, 1997.

The first part of the chapter discusses the importance of the

second part of the chapter discusses the importance of the

third part of the chapter discusses the importance of the

fourth part of the chapter discusses the importance of the

fifth part of the chapter discusses the importance of the

sixth part of the chapter discusses the importance of the

seventh part of the chapter discusses the importance of the

eighth part of the chapter discusses the importance of the

ninth part of the chapter discusses the importance of the

tenth part of the chapter discusses the importance of the

eleventh part of the chapter discusses the importance of the

twelfth part of the chapter discusses the importance of the

thirteenth part of the chapter discusses the importance of the

BIBLIOGRAPHY

- Bailey, A. and S. Murray, *Explosives, Propellants and Pyrotechnics*, Brasseys, Inc, 1989.
- Bening, R. and M. Kurtz Jr, *The Formation of a Crater as Observed in a Series of Laboratory-scale cratering experiments*, U.S. Army Engineer Nuclear Cratering Group, 1967.
- Bowen, J., Manson, N., Oppenheim, A., and R. Soloukhin, *Shock Waves, Explosions, and Detonations*, American Institute of Aeronautics and Astronautics, Inc., 1983.
- Chew, T., Rooke, A. Jr., and L. Pitman, *A Small-scale Study of Craters Resulting from Repeated Explosions along a Common Vertical Axis*, Waterways Experiment Station, 1968.
- Cooper, P. and S. Kurowski, *Introduction to the Technology of Explosives*, VCH Publishers, Inc, 1966.
- Dobratz, M., *LLNL Explosives Handbook: Properties of Chemical Explosives and Explosive Simulants*, Lawrence Livermore Laboratory, University of California, 1981.
- Enhamre, Z., *Effects of Underwater Explosions on Elastic Structures in Water*, Bulletin No. 42, Transactions of the Royal Institute of Technology, 1954.
- Kuhl, A., Leyer, J., Borisov, A., and W. Sirignano, *Dynamic Aspects of Detonations. Volume 153, Progress in Astronautics and Aeronautics*, American Institute of Aeronautics and Astronautics, Inc., 1993.
- Gibbs, T. and A. Popolato, *LASL Explosive Property Data*, University of California Press, 1980.
- Graham, R., *Solids under High Pressure Shock Compression*, Springer-Verlag, N.Y. 1992.
- Rooke, A. Jr, Carnes, B., and L. Davis, *Cratering by Explosions: A compendium and an Analysis*, Waterways Experiment Station, 1974.
- Rooke, A. Jr. and T. Chew, *Crater and Ejecta Measurements for a full-scale Missile Detonation in an Underground cell*, Waterways Experiment Station, 1966.
- Rooke A. Jr. and J. Strange. *Techniques for Determining the Cratering Effects of Surface and Underground Explosions*, Waterways Experiment Station, 1966.

Snell, C., *One-dimensional analysis: Shock Wave Propagation from Underwater Cratering Detonations*, Waterways Experiment Station, 1975.

Spyrakos, C., *Finite Element Modeling in Engineering Practice*, West Virginia University Press, 1994.

Wolsky, S. and A. Czanderna, *Ballistic Materials and Penetration Mechanics*, Elsevier Scientific Publishing Company, 1980.

Zukas, J., Nicholas, T., Swift, H., Greszczuk, L., and D. Curran, *Impact Dynamics*, Wiley-Interscience Publication, 1982.

INITIAL DISTRIBUTION LIST

1. Defense Technical Information Center.....2
8725 John Kingman Rd., Ste 0944
Ft. Belvoir, Virginia 22060-6218

2. Dudley Knox Library.....2
Naval Postgraduate School
411 Dyer Rd.
Monterey, California 93943-5101

3. Defense Logistics Studies Information Exchange.....1
U.S. Army Logistics Management College
Fort Lee, Virginia 23801-6043

4. Chairman, Department of Physics.....1
Professor William Maier
Naval Postgraduate School
Monterey, California 93943

5. Professor Xavier Maruyama, Code PH Mx.....3
Department of Physics
Monterey, California 93943

6. Sandia National Laboratories.....2
Attn: Dr. Ronald Woodfin
Exploratory Sensors and Fuzing Department
Sandia National Laboratories
Albuquerque, New Mexico 87185-0860

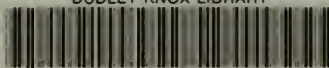
7. Defense Technical Information Center.....1
ATTN: Selection Section (DTIC-FDAC)
Building 5, Cameron Station
Alexandria, Virginia 22304-6145

8. PEO Mine Warfare.....1
PMS-407-DB
Attn: LTC Dan Brush
2531 Jefferson Davis Highway
Arlington, Virginia 22242-5167

| | | |
|----|----------------------------|---|
| 9. | CPT Albert L. Alba..... | 2 |
| | Naval Postgraduate School | |
| | Monterey, California 93943 | |

DUDLEY KNOX LIBRARY
NAVAL POSTGRADUATE SCHOOL
MONTEREY CA 93943-5101

DUDLEY KNOX LIBRARY



3 2768 00343997 7